

# REPORT BACK ALTERNATIVES

---

R. Rückl (Würzburg)

---

WG Conveners : Graham Wilson (E)  
Michael Spira (T)  
Reinhold Rückl (T)

# TDR David Miller

•  
•  
•

WORK  
needed

## ■ HIGGS MECHANISM

→ wide and invisible H

## ■ SUPERSYMMETRY

→  $\tilde{X}$ -processes

$\tilde{\nu}_e$ -res.

## ■ ALTERNATIVES

strong WW interactions

$WW \rightarrow t\bar{t}$

compositeness

LQ, CI?

large extra dimensions

missing!

## ■ HIGH PRECISION PHYSICS

→ LFV in Z decays

→ extended gauge sym. ( $W', Z', E, N$ )

•  
•  
•

introduction  
 $e^+e^-$

# ALTERNATIVES

Kilian  
Zerwas

## 2.2.1 Strong interactions of electroweak gauge bosons

Unitarity leads to the alternative that either a light Higgs boson is realized in the electroweak sector of the Standard Model, or the electroweak  $W^\pm, Z$  gauge bosons become strongly interacting at high energies [1]. The second scenario, compatible with the high-precision electroweak data, can be analyzed in quasi-elastic scattering of  $W^\pm, Z$  bosons,

$$WW \rightarrow WW \quad (1)$$

at TeV  $e^+e^-$  linear colliders [2].

The strong interactions of the  $W$  bosons at high energies can be traced back, in a natural way, to the dynamics of Goldstone bosons which are associated with the spontaneous breaking of a chirally invariant theory, characterized by an energy scale  $\Lambda_* \sim \mathcal{O}(1 \text{ TeV})$ . This theory can be described by an effective Lagrangian, expanded in the dimensions of the interaction terms [3]:

$$\mathcal{L} = \mathcal{L}_2 + \mathcal{L}_0 + \mathcal{L}_4 + \mathcal{L}_5 + \dots \quad (2)$$

$\mathcal{L}_2$  denotes the kinetic terms of the gauge fields while  $\mathcal{L}_0$ , the lowest-order term in the chiral expansion, corresponds to the mass term:

$$\begin{aligned} \mathcal{L}_2 &= -\frac{1}{8} \text{Tr} [W_{\mu\nu}^2] - \frac{1}{4} B_{\mu\nu}^2 \\ \mathcal{L}_0 &= M_W^2 W_\mu^+ W_\mu^- + \frac{1}{2} M_Z^2 Z_\mu Z_\mu \end{aligned} \quad (3)$$

These two terms generate the parameter-free  $WW$  scattering amplitudes in the threshold region of the strong-interaction domain. The dimension-4 operators  $\mathcal{L}_4$  and  $\mathcal{L}_5$  are new quadrilinear contact interactions of the  $W^\pm$  and  $Z$  bosons:

$$\begin{aligned} \mathcal{L}_4 &= \alpha_4 [\text{Tr}(V_\mu V_\nu)]^2 \\ \mathcal{L}_5 &= \alpha_5 [\text{Tr}(V_\mu V_\mu)]^2 \end{aligned} \quad (4)$$

with  $V_\mu = i(gW_\mu - g'\tau_3 B_\mu)/2$  in standard notation. The coefficients  $\alpha_4$  and  $\alpha_5$  are parameters which describe the dynamics of the new strong interactions.

The amplitudes for the quasi-elastic  $WW$  scattering processes,

$$\begin{aligned} A(W^+W^- \rightarrow ZZ) &= A(s, t, u) \\ A(W^+W^- \rightarrow W^+W^-) &= A(s, t, u) + A(t, s, u) \\ A(W^-W^- \rightarrow W^-W^-) &= A(t, s, u) + A(u, t, s) \end{aligned} \quad (5)$$

can be expressed in terms of a master amplitude  $A$  which is a function of the Mandelstam variables,

$$A(s, t, u) = \frac{s}{v^2} + \alpha_4 \frac{4(t^2 + u^2)}{v^4} + \alpha_5 \frac{8s^2}{v^4} + \dots \quad (6)$$

with  $v = 1/[\sqrt{2}G_F]^{1/2} = 246 \text{ GeV}$ . The leading-order term  $s/v^2$  reflects the parameter-independent approach to the strong-interaction domain of the  $W$  bosons.

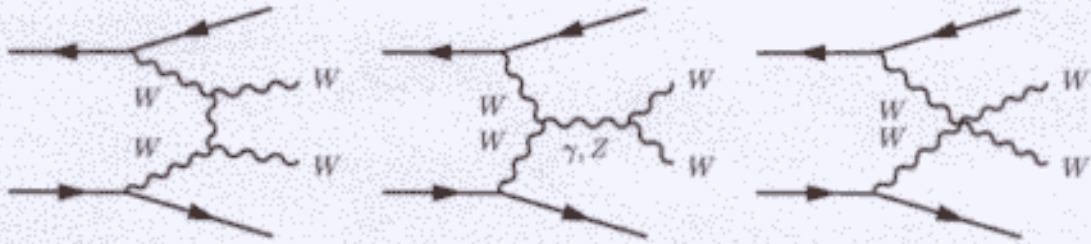


Figure 2: Generic diagrams contributing to the strong  $WW$  scattering signal.

The  $WW$  scattering processes can be analyzed experimentally in high energy  $e^\pm e^-$  collisions in which the initial-state  $W^\pm$  bosons are generated as quasi-real particles:

$$e^+e^- \rightarrow \bar{\nu}\nu W^+W^- \quad \text{and} \quad \bar{\nu}\nu ZZ \quad (7)$$

$$e^-e^- \rightarrow \nu\nu W^-W^- \quad (8)$$

The theoretical analysis of these reactions involves the signal diagrams of Fig.2, to be complemented by background diagrams which account for  $\gamma\gamma \rightarrow WW$  subprocesses,  $W$  radiation off lepton lines, *etcetera*.

The strategy for isolating the signal from the background has been described in detail in Ref. [2]. In the present analysis the following cuts have been applied:

$$\mathcal{C}: M(\nu\bar{\nu}) > 150 \text{ GeV}$$

$$|\cos \theta(W/Z)| < 0.8 \text{ and } p_\perp(W/Z) > 100 \text{ GeV}$$

$$p_\perp(WW) > 40 \text{ GeV} \text{ resp. } p_\perp(ZZ) > 30 \text{ GeV}$$

$$400 \text{ GeV} < M(WW/ZZ) < 800 \text{ GeV}$$

Taking into account leptonic and hadronic decays of the  $W^\pm$  and  $Z$  bosons, overall detection efficiencies of 33% for both  $WW$  and  $ZZ$  pairs can be reached. The  $e^\pm e^-$  c.m. energy has been set  $\sqrt{s} = 1 \text{ TeV}$  and the integrated luminosities  $\int \mathcal{L}[e^+e^-] = 1 \text{ ab}^{-1}$  and  $\int \mathcal{L}[e^-e^-] = 100 \text{ fb}^{-1}$  have been assumed for the high-luminosity operation of the collider. Electron and positron polarizations are assumed to be 100 % and 50 %, respectively.

The results of this analysis are summarized in Fig.3. Exclusion contours at the  $1\sigma$  level are shown for the parameters  $[\alpha_4, \alpha_5]$  as derived from the three processes introduced above. The highest sensitivity is predicted for the  $W^+W^-$  and  $ZZ$  channels; the additional  $W^-W^-$  channel, however, is useful for resolving the two-fold ambiguity and singling out the unique solution. For an energy of 1 TeV and luminosities as specified above, the dynamical parameters  $\alpha_4$  and  $\alpha_5$  can be measured to an accuracy  $\alpha_4 \lesssim 0.010$  and  $\alpha_5 \lesssim 0.007$ .

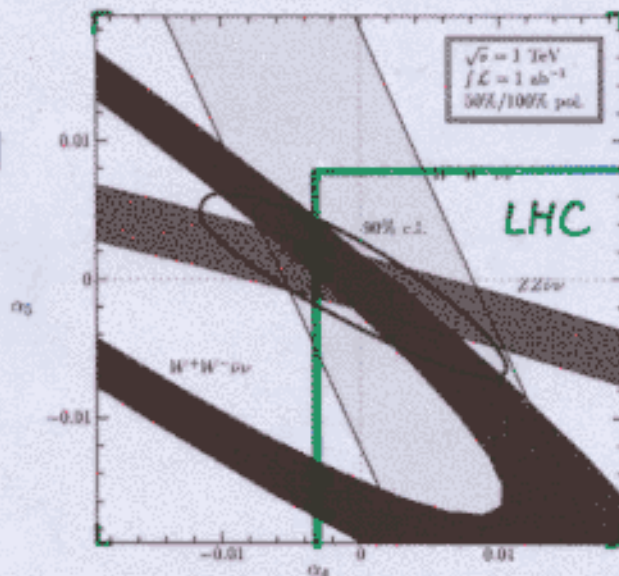
Bounds on the parameters  $\alpha_4$  and  $\alpha_5$  from LHC analyses [4] are expected to be about a factor three less stringent for the equivalent luminosity after two years of operation.

The sensitivity bounds on  $\alpha_{4,5}$  can be rephrased in bounds on the new strong-interaction scale  $\Lambda_*$  which can be probed in these experiments. Defining  $\min[\alpha_i] = v^2/\Lambda_*^2$ , the bounds derived above can be translated to

$$\Lambda_* \gtrsim 3 \text{ TeV} \quad (9)$$

Resonance effects of the new strong interactions are expected at scales  $\sim 4\pi v = 3 \text{ TeV}$ . As a result, the entire threshold region of the  $WW$  strong interactions can be covered at the high-luminosity  $e^+e^-$  collider TESLA.

will be replaced  
by exp. study



$$\begin{aligned} \sqrt{s} &= 1 \text{ TeV} \\ \int \mathcal{L}_{e^+e^-} &= 1 \text{ ab}^{-1} \\ P_{e^-} &= 1 \\ P_{e^+} &= 0.5 \end{aligned}$$

Figure 3: Exclusion contours for the hypothesis  $\alpha_{4,5} = 0$ , assuming  $\sqrt{s} = 1 \text{ TeV}$  and an integrated  $e^+e^-$  luminosity of  $\int \mathcal{L} = 1 \text{ ab}^{-1}$  (50%/100% polarization). The 90% exclusion line has been obtained by combining the  $W^+W^-$  and  $ZZ$  channels (dark gray). The contour for the  $W^-W^-$  channel (light gray) corresponds to an integrated  $e^-e^-$  luminosity of  $\int \mathcal{L} = 100 \text{ fb}^{-1}$  (100% polarization).

## References

- [1] C.H. Llewellyn Smith, Phys. Lett. **B46**, 233 (1973); B. Lee, C. Quigg and H. Thacker, Phys. Rev. Lett. **38**, 883 (1977); Phys. Rev. **D16**, 1519 (1977).
- [2] E. Boos, H.-J. He, W. Kilian, A. Pukhov, C.-P. Yuan, and P.M. Zerwas, Phys. Rev. **D57**, 1553 (1998) and Phys. Rev. **D61**, 077901 (2000).
- [3] T. Appelquist and C. Bernard, Phys. Rev. **D22**, 200 (1980); A. Longhitano, Phys. Rev. **D22**, 1166 (1980); Nucl. Phys. **B188**, 118 (1981); T. Appelquist and G.-H. Wu, Phys. Rev. **D48**, 3235 (1993); M. Veltman, Report CERN 97-05.
- [4] A.S. Belyaev, O. Eboli, M.C. Gonzalez-Garcia, J.K. Mizukoshi, S.F. Novaes, and I. Zacharov, Phys. Rev. **D59**: 15022 (1999).

! still missing:  $e^+e^- \rightarrow \bar{\nu}\nu \bar{t}t$  ( $WW \rightarrow \bar{t}t$ )

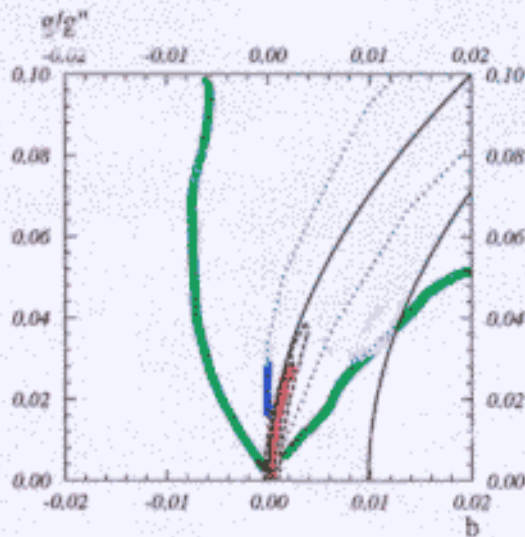
# ALTERNATIVES : Compositeness

## 2.3.2 Vector resonances and pseudo-Goldstone bosons from a strong EW sector *Casalbuoni et al.*

We have considered two possible realizations of a dynamical EW symmetry breaking scenario which predict new vector resonances: BESS [1] and degenerate BESS [2]. The model BESS is an effective description for dynamical symmetry breaking, and it includes for instance most of the usual technicolor models. The model degenerate BESS describes strong axial vector and vector resonances almost degenerate in mass. The parameters of the BESS model are the mass of the new  $SU(2)$  gauge bosons  $M_V$ , their self coupling  $g''$ , and a third parameter  $b$  whose strength characterizes the direct couplings of the new vectors  $V$  to the fermions. For the BESS model the  $W^+W^-$  channel is the dominant one, while for the degenerate BESS model, the best channel for discovery is  $ff$  [2]. Our analysis, in the fermion channels, is based on the following observables:  $\sigma^h$ ,  $\sigma^b$ ,  $A_{PB}^{e^+e^- \rightarrow \mu^+\mu^-}$ ,  $A_{FB}^{e^+e^- \rightarrow b\bar{b}}$ ,  $A_{LR}^{e^+e^- \rightarrow \mu^+\mu^-}$ ,  $A_{LR}^{e^+e^- \rightarrow b\bar{b}}$ ,  $A_{LR}^{e^+e^- \rightarrow had}$  (with  $P_e = 0.8$ ). Concerning the  $WW$  channel, we have studied the following observables:  $\frac{d\sigma}{d\cos\theta}(e^+e^- \rightarrow W^+W^-)$ ,  $A_{LR}^{e^+e^- \rightarrow W^+W^-}$ , the longitudinal and transverse polarized  $W$  differential cross sections and asymmetries. The bounds from a

V

mainly  $e^+e^- \rightarrow W^+W^-$



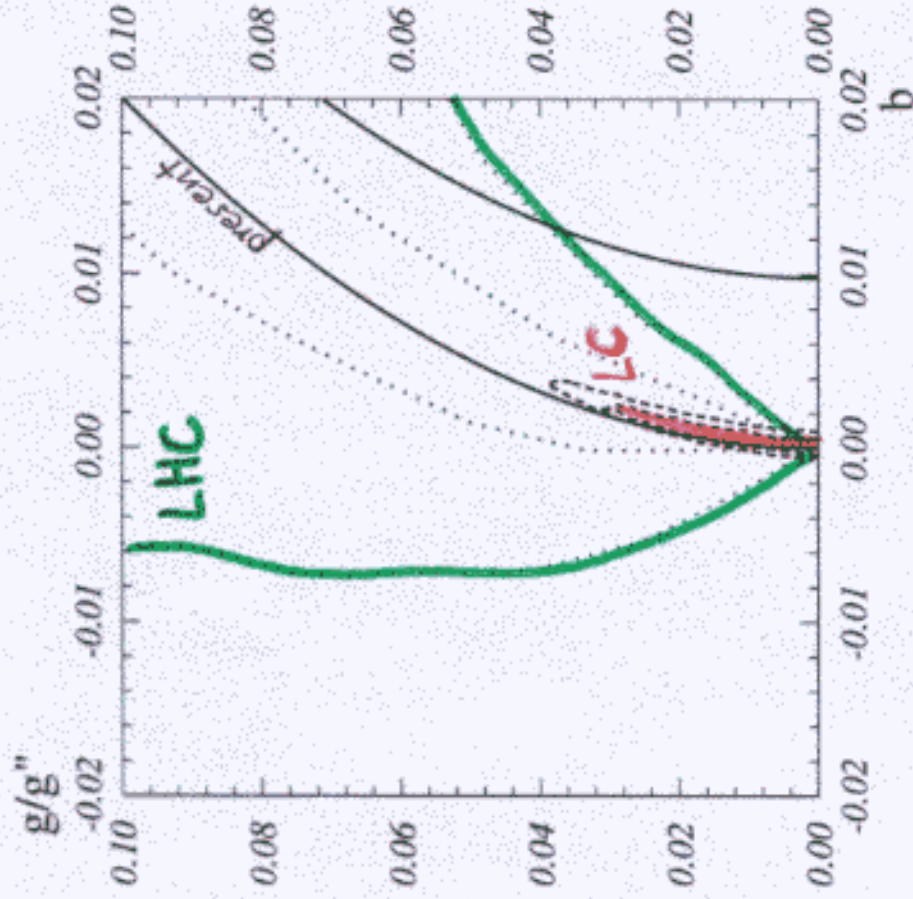
only 2 TeV will be shown

Figure 4: 95%CL bounds for the BESS model from the present EW data (solid), from LHC for  $M_V = 1 TeV$  (inner dot) and for  $M_V = 2 TeV$  (outer dot), from LC at  $\sqrt{s} = 500 GeV$ ,  $L = 1000 fb^{-1}$ ,  $M_V = 1 TeV$  (outer dash) and at  $\sqrt{s} = 800 GeV$ ,  $L = 1000 fb^{-1}$ ,  $M_V = 2 TeV$  (inner dash). The allowed regions are the internal ones.

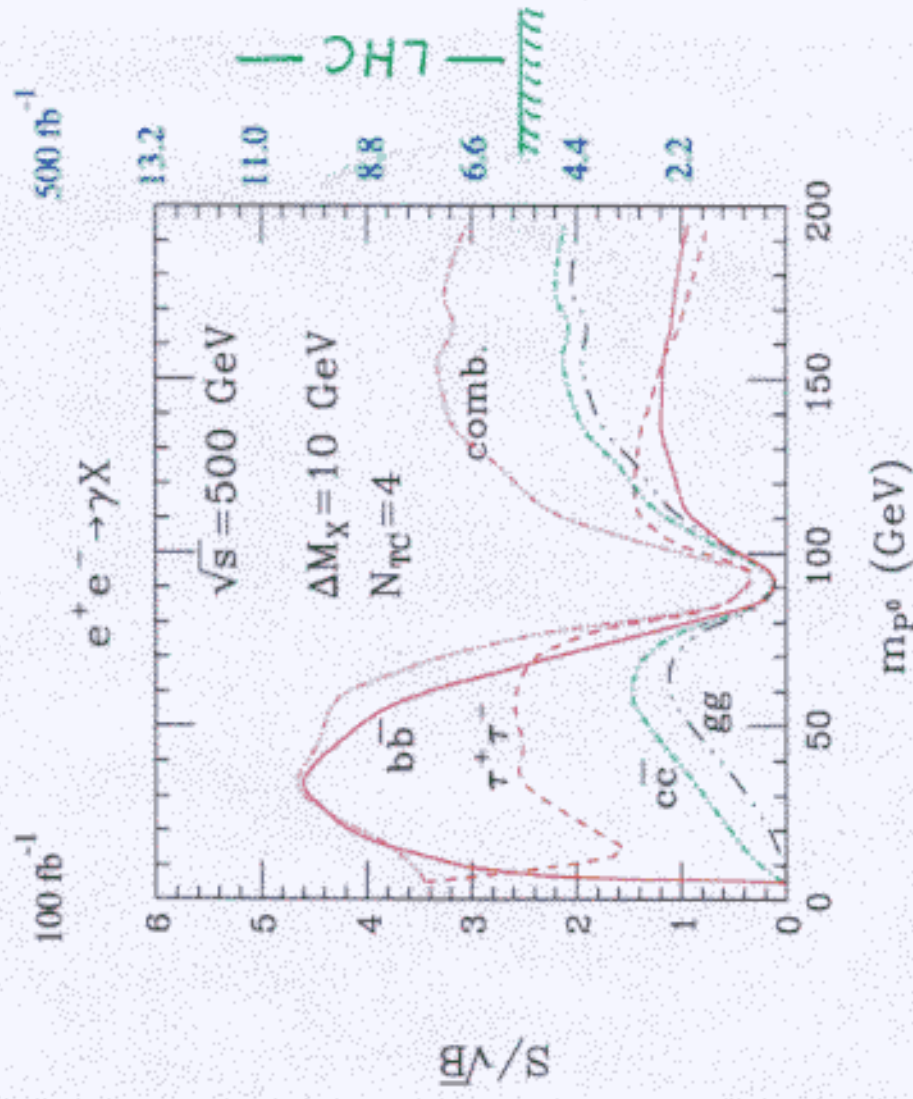
LC, obtained by combining all the observables, are shown in Fig. 4 for the BESS model. In conclusion, linear colliders in the considered ranges are found to be even more efficient than LHC.

In the case of degenerate BESS, LHC seems to be superior for testing the model when compared with the proposed linear colliders at the energies and luminosities considered. However, by assuming that a neutral resonance has been seen at the LHC with a mass below 1

$$M_V = 2 \text{ TeV}$$



$$\sqrt{s} = 800 \text{ GeV}, 1 \text{ ab}^{-1}$$



$$\text{LHC} (gg \rightarrow P^0 \rightarrow \gamma\gamma), 150 \text{ fb}^{-1}$$

$TeV$ , then the future LC could be able to study it, and, in particular, if the energy spread of the beams is sufficiently small, to split the two nearly degenerate resonances and measure their widths [3]. For example, considering a spread in the c.o.m. energy given by  $\sigma_E \sim 0.007R(\%)E$ , for  $R = 1\%$ , one can split the two resonances for  $g/g'' \geq 0.16$  [3].

Theories of the EW interactions based on dynamical symmetry breaking avoid the introduction of fundamental scalar fields but generally predict many pseudo-Nambu-Goldstone bosons (PNGB's) due to the breaking of a large initial global symmetry group  $G$ . In the broad class of models considered in [4], the lightest neutral PNGB  $P^0$  is of particular interest. At the LHC, the  $gg \rightarrow P^0 \rightarrow \gamma\gamma$  channel provides an extremely robust detection mode. For  $N_{TC} = 4$ ,  $S/\sqrt{B} \geq 5$  for  $L = 10 fb^{-1}$  ( $L = 150 fb^{-1}$ ) in the range  $50 \leq m_{P^0} \leq 150 GeV$  (at least  $30 \leq m_{P^0} \leq 200 GeV$ , the upper mass reach probably being considerably higher). Even for the unrealistically low value of  $N_{TC} = 1$ ,  $S/\sqrt{B} \geq 5$  for  $L = 150 fb^{-1}$  and  $70 \leq m_{P^0} \leq 150 GeV$ . At the Tevatron, for  $N_{TC} = 4$  the  $gg \rightarrow P^0 \rightarrow \gamma\gamma$  mode yields  $S/\sqrt{B} \geq 3 \times (L/2 fb^{-1})^{1/2}$  for  $60 \leq m_{P^0} \leq 200 GeV$ . At the LHC and Tevatron,  $P^0$  detection in its (main)  $b\bar{b}$  decay mode would be difficult. The best mode for  $P^0$  production at a

(P)

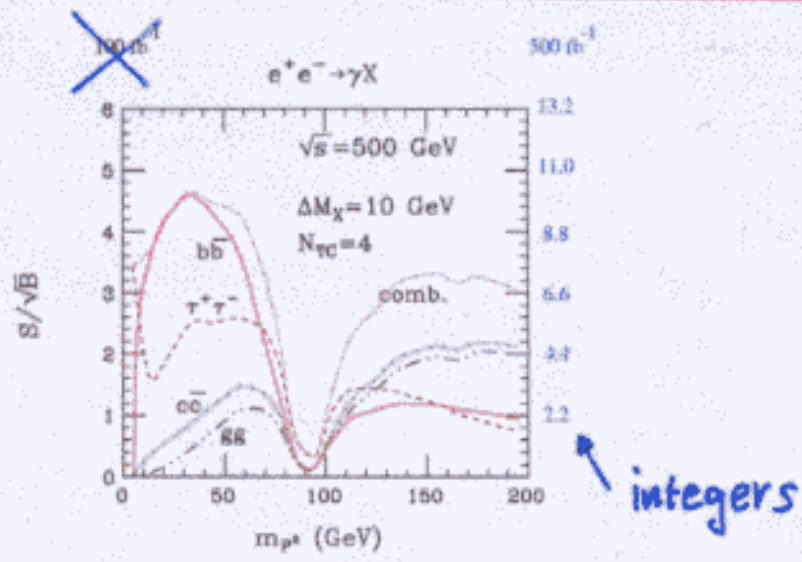


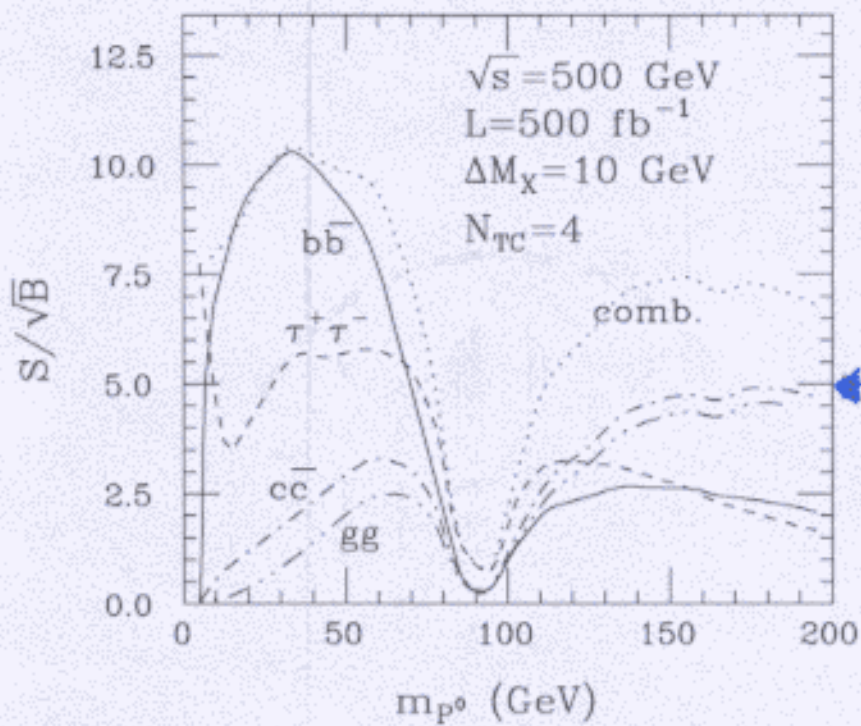
Figure 5: The statistical significances  $S/\sqrt{B}$  for a  $P^0$  signal in various 'tagged' channels as a function of  $m_{P^0}$  at a 500 GeV collider for integrated luminosities of  $100 fb^{-1}$  and  $500 fb^{-1}$ .

LC is  $e^+e^- \rightarrow \gamma P^0$ . Results for  $S/\sqrt{B}$ , in the various tagged channels, for  $N_{TC} = 4$  and assuming  $L = 100 fb^{-1}$  (and  $L = 500 fb^{-1}$ ) at  $\sqrt{s} = 500 GeV$ , are plotted in Fig. 5 [4]. Also shown is the largest  $S/\sqrt{B}$  that can be achieved by considering all possible combinations of the  $gg$ ,  $c\bar{c}$ ,  $b\bar{b}$  and  $\tau^+\tau^-$  channels. We find  $S/\sqrt{B} \geq 3 \times (N_{TC}/4)^2 \times (L/100 fb^{-1})^{1/2}$  for  $m_{P^0} \leq 75 GeV$  and  $m_{P^0} \geq 130 GeV$ . For  $N_{TC} = 4$  and  $L = 100 fb^{-1}$ , a strong signal,  $S/\sqrt{B} \sim 4$ , is only possible for  $m_{P^0} \sim 20 - 60 GeV$ . For the TESLA  $L = 500 fb^{-1}$  luminosity option, discovery prospects are clearly improved;  $P^0$  discovery might even be possible for  $N_{TC} < 4$ . Unlike the LHC, for high enough  $L$  the LC can potentially probe quite low values of  $m_{P^0}$  and could measure ratios of a number of interesting  $P^0$  decay modes. The  $\gamma\gamma$  option at an  $e^+e^-$  collider is actually a more robust means for discovering the  $P^0$  than direct

$\frac{S}{\sqrt{B}}$  vs  $m_{P^0}$   $\gamma\gamma \rightarrow P^0 \rightarrow b\bar{b}$  will be shown + comment on 1Tel

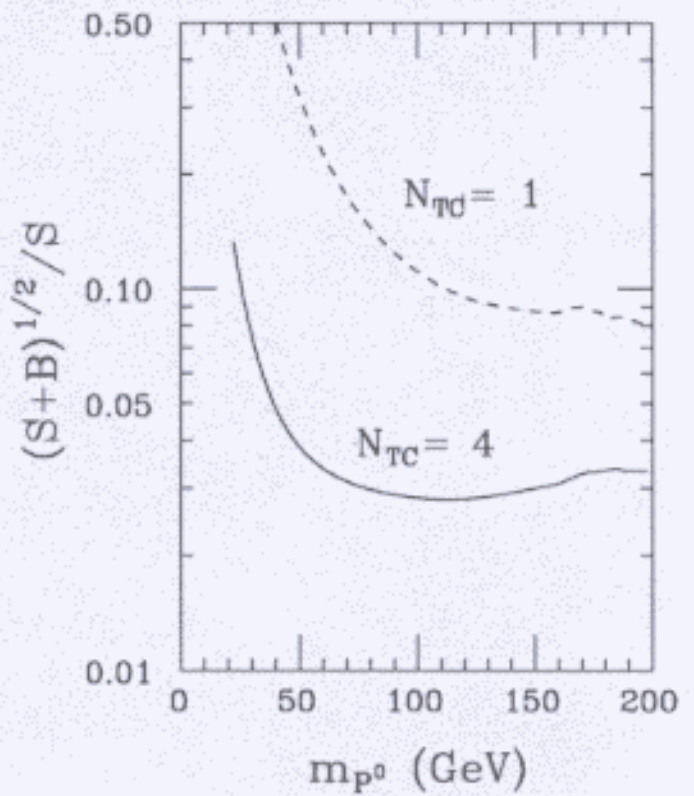
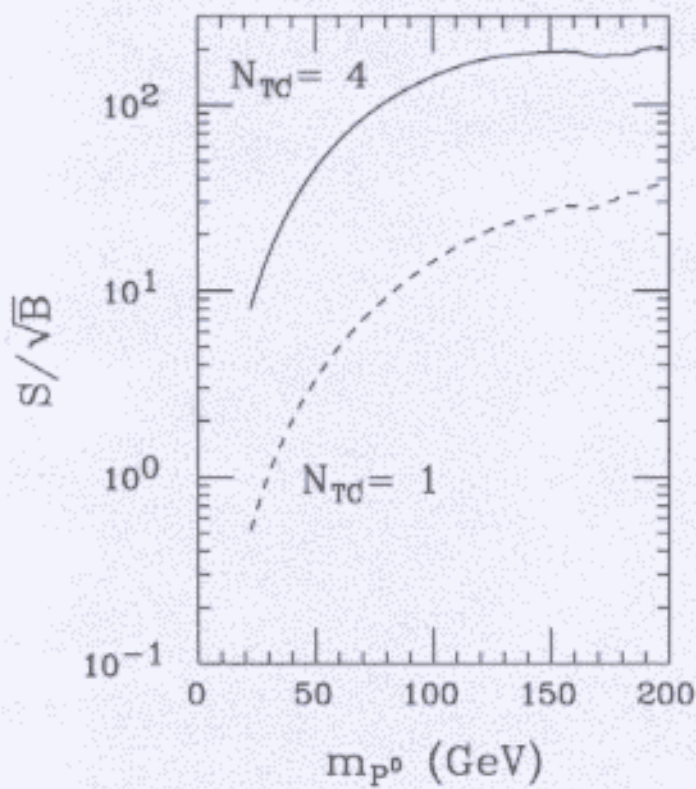


$$e^+e^- \rightarrow \gamma X$$



### $\gamma\gamma \rightarrow b\bar{b}$ Signal

$L_{\text{eff}}=20\text{fb}^{-1}$ ,  $z_0=0.85$ ,  $\langle\lambda\lambda'\rangle=0.8$ ,  $\Gamma_{\text{exp}}=5\text{ GeV}$



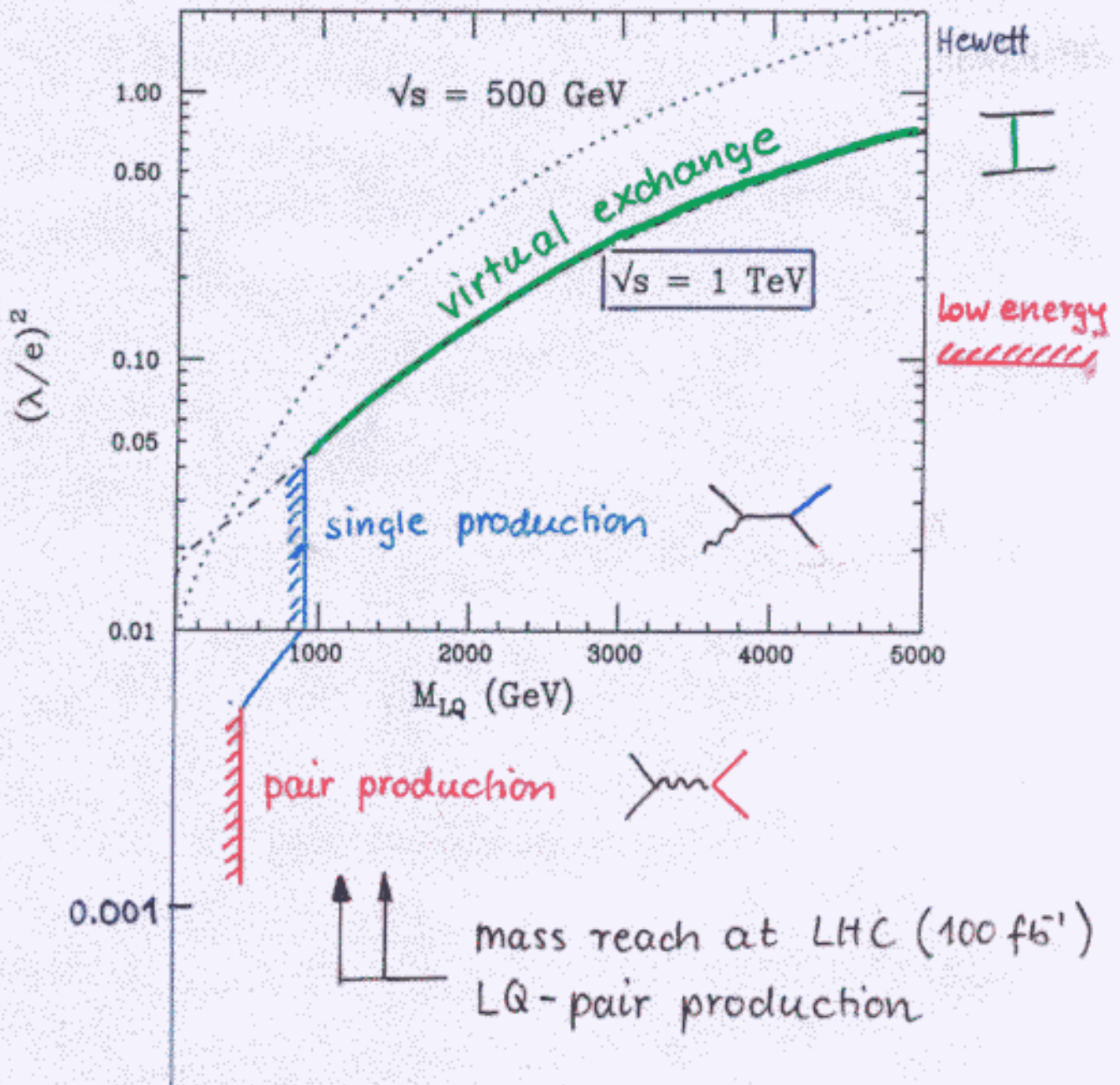
superior to LHC !

operation in the  $e^+e^-$  collision mode. For  $N_{TC} = 4$  and using a set-up with a broad  $E_{\gamma\gamma}$  spectrum, a  $P^0$  signal should be easily detectable in  $\gamma\gamma \rightarrow P^0 \rightarrow b\bar{b}$  for  $0.1 \leq \frac{m_{P^0}}{m_b} \leq 0.7$  with minimal luminosity ( $L_{eff} \sim 20 \text{ fb}^{-1}$ ). Once  $m_{P^0}$  is known, the  $\gamma\gamma$  collision set-up can be re-configured to yield a luminosity distribution that is strongly peaked at  $E_{\gamma\gamma} \sim m_{P^0}$  and, for much of the mass range of  $m_{P^0} \leq 200 \text{ GeV}$ , a measurement of  $\Gamma(P^0 \rightarrow \gamma\gamma)B(P^0 \rightarrow b\bar{b})$  can be made with statistical accuracy in the  $\sim 2\%$  range [4].

## References

- [1] R.Casalbuoni, S.De Curtis, D.Dominici and R.Gatto, Phys. Lett. **B155**, (1985) 95, Nucl. Phys. **B282**, (1987) 235.
- [2] R.Casalbuoni, A.Deandrea, S.De Curtis, D.Dominici, F.Feruglio, R.Gatto and M.Grazzini, Phys. Lett. **B349** (1995) 533; R.Casalbuoni, A.Deandrea, S.De Curtis, D.Dominici, R.Gatto and M.Grazzini, Phys. Rev. **D53** (1996) 5201.
- [3] R.Casalbuoni, A.Deandrea, S.De Curtis, D.Dominici, R.Gatto and J.F.Gunion, JHEP 9908:011, 1999.
- [4] R. Casalbuoni, A. Deandrea, S. De Curtis, D. Dominici, R. Gatto and J. F. Gunion, Nucl. Phys. **B555** (1999) 3; LC-TH-1999-013, Oct 1999, hep-ph/9912333

# summary of LQ searches at $e^+e^-$ Linear Colliders

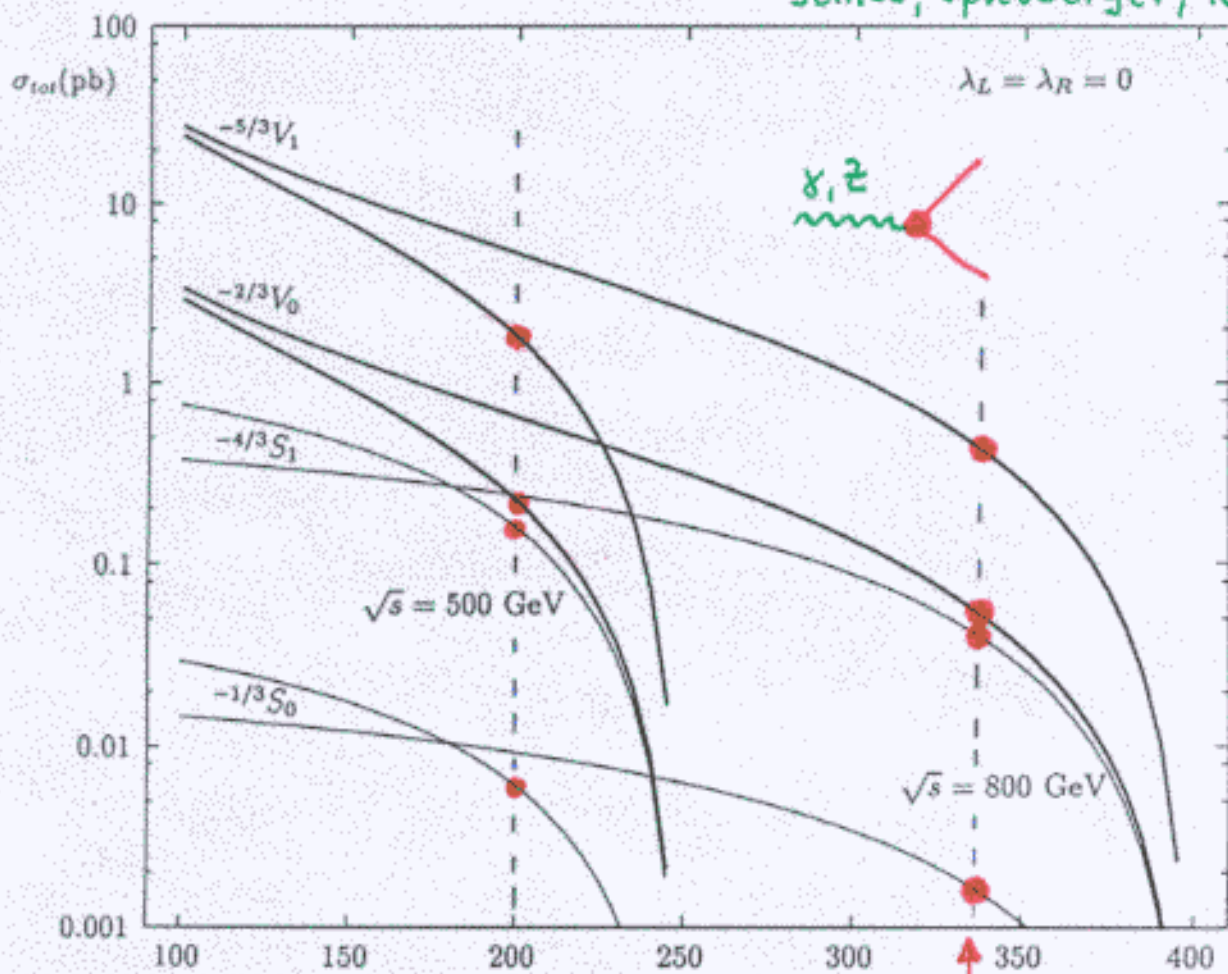


⇒ most likely discovered at LHC

LC can elucidate quantum numbers

spin / weak isospin

Settles, Spiessberger, RR



mass known

not possible in  $\bar{p}p$  and  $e p$  searches

↑  
color

↑  
Yukawa

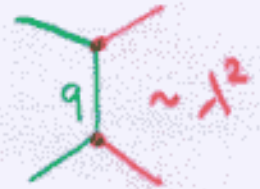
scalar LQs    charge    ew

$\Phi_s$	$Q_\Phi^I$	$T_3$	$Q_\Phi^Z$	#	$\delta Q_\Phi^I$	$\delta Q_\Phi^Z$
$S_1$	1/3	0	-0.182	545	$\pm 0.008$	+0.07 - 0.04
$\tilde{S}_1$	4/3	0	-0.729	8713	$\pm 0.008$	$\pm 0.05$
$S_3^u$	4/3	1	1.648	13783	$\pm 0.009$	$\pm 0.02$
$S_3^0$	1/3	0	-0.182	545	$\pm 0.008$	+0.07 - 0.04
$S_3^d$	-2/3	-1	-2.012	9448	$\pm 0.014$	$\pm 0.01$
$R_2^u$	5/3	1/2	0.277	13232	$\pm 0.007$	-0.07 + 0.06
$R_2^d$	2/3	-1/2	-1.552	5644	$\pm 0.015$	$\pm 0.01$
$\tilde{R}_2^u$	2/3	1/2	0.824	3446	$\pm 0.009$	$\pm 0.02$
$\tilde{R}_2^d$	-1/3	-1/2	-1.006	2362	$\pm 0.014$	$\pm 0.01$

Blümlein

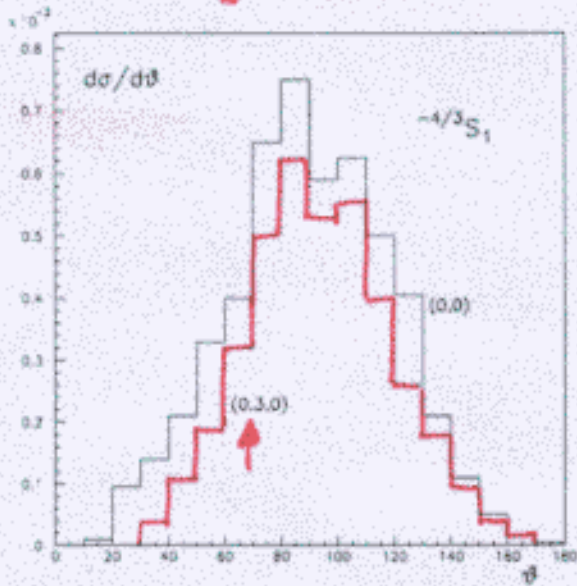
↑  
 $\sqrt{s} = 1 \text{ TeV}$ ,  $\int \mathcal{L} = 300 \text{ fb}^{-1}$   
 $M_\phi = 400 \text{ GeV}$   
 statistical errors only

# Yukawa coupling

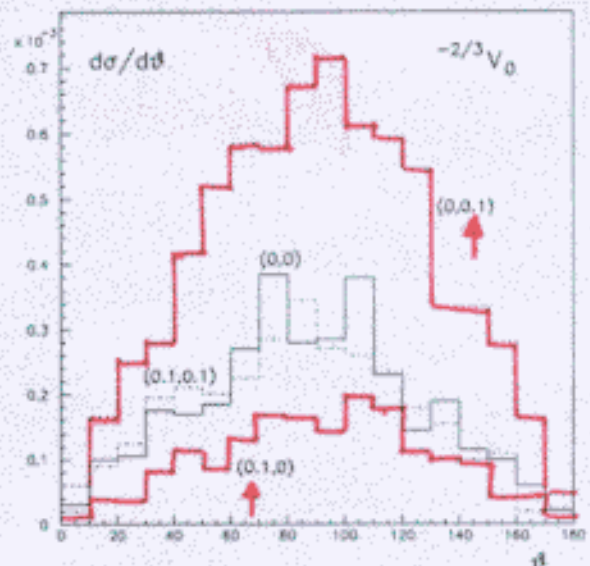


$$\lambda_L = 0.0909$$

$$\lambda_{L,R} = 0.03$$

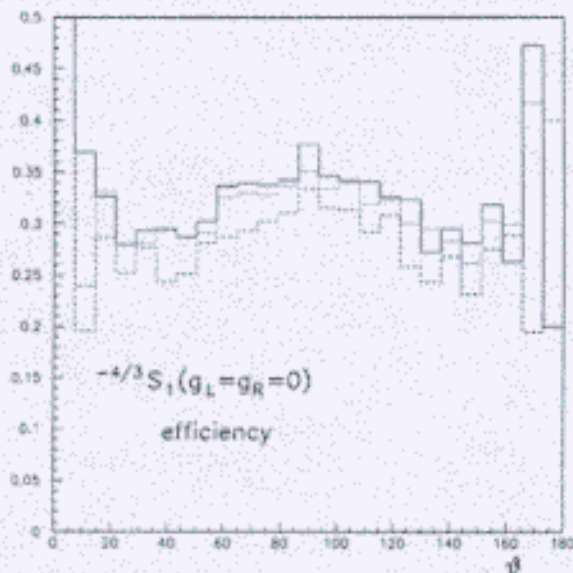


(a)

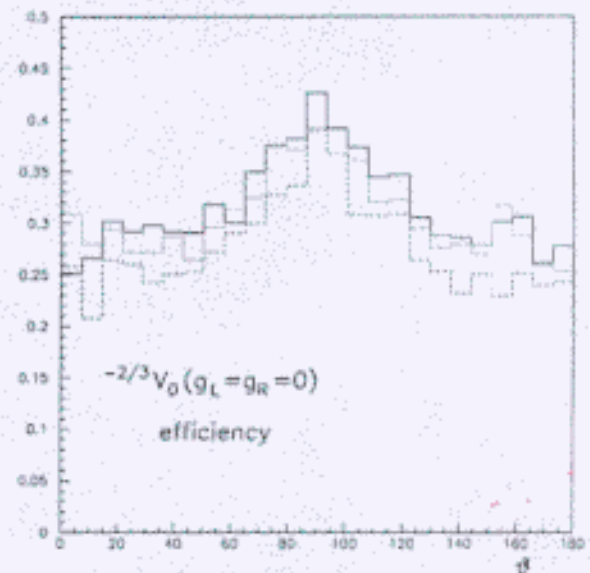


(b)

Figure 7: Angular dependence of the production cross sections for (a)  $-4/3 S_1$  and (b)  $-2/3 V_0$  for various Yukawa couplings  $(g_L, g_R)$  in units of  $e$  ( $M = 300 \text{ GeV}$ ,  $\sqrt{s} = 800 \text{ GeV}$ ,  $\mathcal{L} = 50 \text{ fb}^{-1}$ , cuts included).



(a)



(b)

Figure 8: Angular dependence of the detection efficiency for a scalar (a) and a vector (b) leptotau in channel I. The full histogram refers to the 1 TeV detector, the dashed one to a LEP/SLD-type detector. The dotted histogram is obtained with the detector simulation of Ref. [24].

requires accurate unfolding of efficiency!

more direct test:  $e\gamma \rightarrow LQq$  (Zarnke)

# Contact interactions

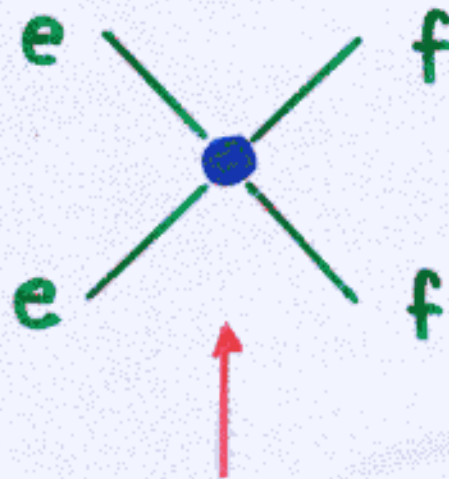
model-independent way to probe

## Alternative New Physics



$E \ll \Lambda$

LC  $\longrightarrow$



$\longleftarrow$  LHC

$\uparrow$  HERA

- \* high sensitivity
- \* polarisation
- \* many channels

topic for the TDR?



$e^+e^- \rightarrow f\bar{f}$  at LC:

interference of virtual  $\gamma$  and Z exchange  
+ interference with NP

$$\frac{d\sigma}{d\cos\theta} \sim \frac{d\sigma(\text{SM})}{d\cos\theta} + \frac{d\sigma(\gamma \otimes NP, Z \otimes NP)}{d\cos\theta} + \frac{d\sigma(NP)}{d\cos\theta}$$

$\sigma(\gamma \otimes NP, Z \otimes NP)$ : main contribution to potential deviations from SM expectations

Already studied:







- ✓ • Z': sensitivity, resolution power
- ✓ • CI: sensitivity (various models, w/o  $e^-$  polarization) : LL, LR, ... AA, VV, .....
- ✓ • LQ,  $\tilde{q}$ : sensitivity above kin. limit
  - extra dim., etc. (to come)
  - details see DESY 123/A...E, Talks & proceedings at workshops and conferences and ref. therein

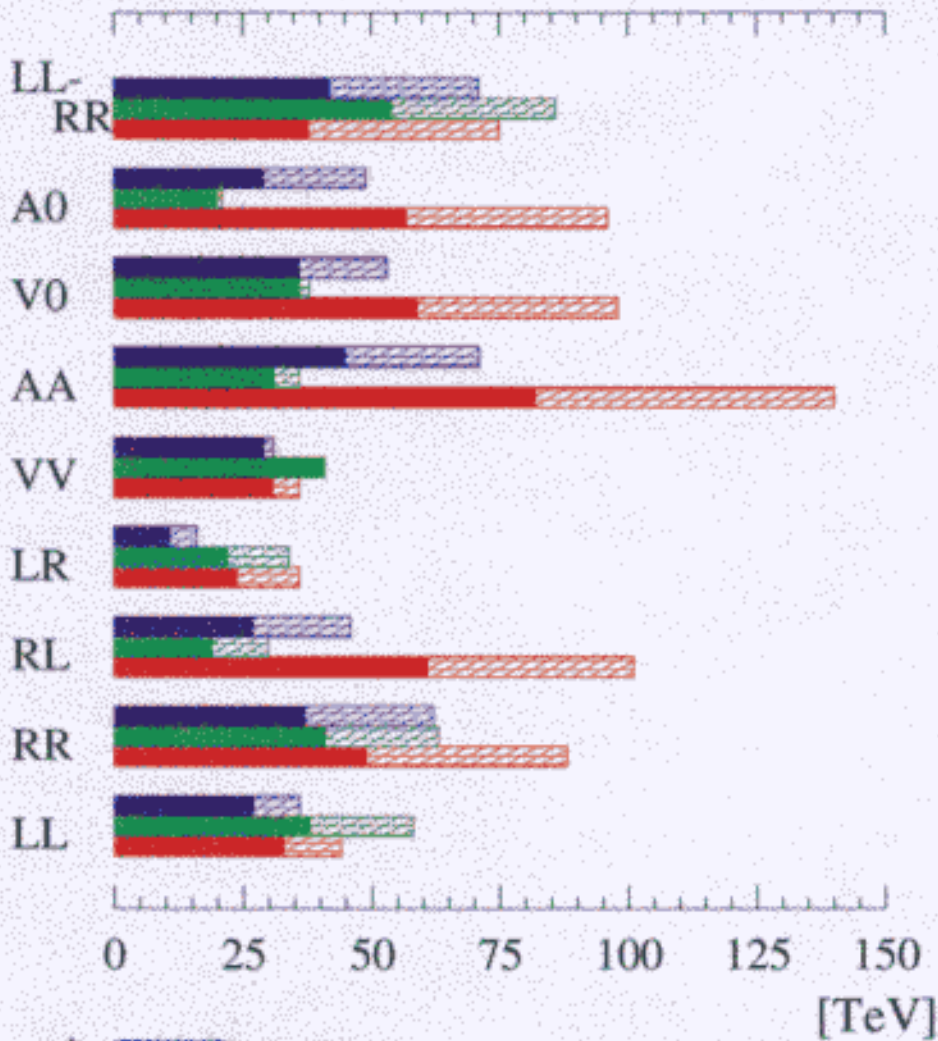
HERE:

- gain with polarization of positrons??
- Comparison with LHC

# Expected Sensitivity from $ee \rightarrow qq$

Comparison w/o  $e^+$  polarization

$500 \text{ fb}^{-1}$ ,  $P_- = 0.8$ ,  $e^+e^- \rightarrow \text{hadrons}$   
 $\Delta_{\text{sys}} = 0.5\%$ ,  $P_+ = 0.6$   $P_+ = 0.0$   
 $ee \rightarrow qq$ :    
 $ee \rightarrow uu$ :    
 $ee \rightarrow dd$ :  



LR, RL, ... +  LHC  
 - 

# Large Extra Dimensions

- attempt to solve hierarchy problem in SM without supersymmetry

$$M_{\text{PL}}^2 = M_0^{2+n} R^n$$

← compactification radius of n dim

↑  
eff. Planck mass  
in 4-dim. world

↑  
fund. Planck mass  
in (4+n)-dim.

$$M_0 = 1 \text{ TeV for } R = \begin{cases} 0.1 \text{ mm} ; & n=2 \\ 10 \text{ \AA} ; & n=3 \end{cases}$$

- inspired by string theory, however little known about compactification
- many variants of model (metric of comp. space fields on brane / in bulk, etc.)
- predict towers of massive Kaluza-Klein states (typically  $m_{\text{KK}} = \frac{k}{R}$ )

## phen. consequences

$$E < \frac{1}{R}$$

heavy states induce higher-dim. operators in  $\mathcal{L}_{\text{eff}}$

$$\frac{1}{R} \ll E$$

light states active

## at LC

$$e^+e^- \rightarrow \gamma + \cancel{G}$$

radiation of KK gravitons

\* sensitive to  $M_0$  and  $n$

$$e^+e^- \rightarrow f\bar{f}$$

exchange of KK gravitons

$$\gamma\gamma \rightarrow WW$$

\* sensitive to  $M_0$  and spin 2

## status

preliminary studies of  $e^+e^- \rightarrow \gamma G$

(Martyn et al., Wilson)

commitment to investigate  $e^+e^- \rightarrow f\bar{f}$

(S. Riemann)

## Generator:

$$e^+e^- \rightarrow \gamma G + \text{ISR} \quad (\text{A. Vest})$$

+ beamstrahlung (CIRCE)

detector-simulation: SIMDET

## Parameters:

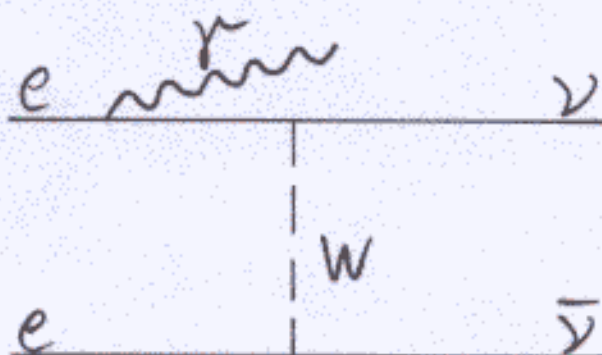
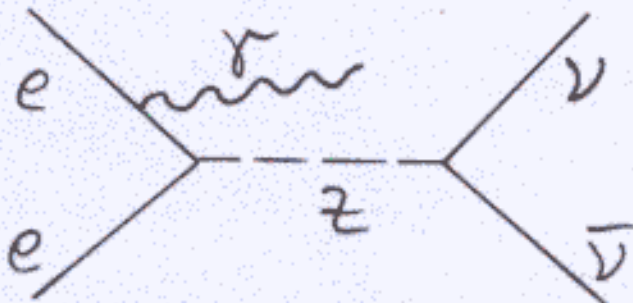
$$\sqrt{s} = 500 \text{ GeV}$$

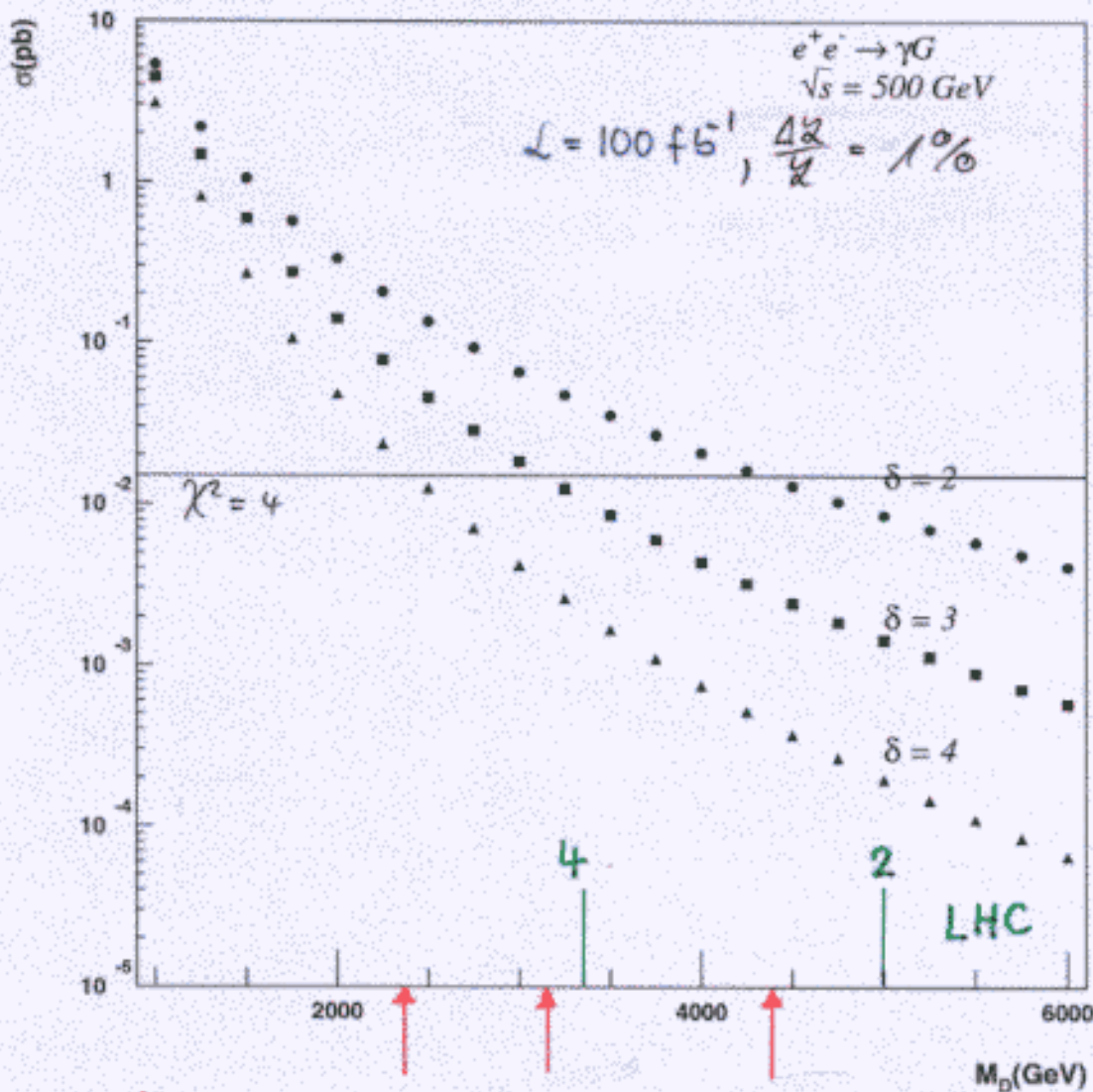
$$\delta = 2, 3, 4$$

$$\mathcal{L} = 100 \text{ fb}^{-1} \quad (500 \text{ fb}^{-1})$$

## background:

$$e^+e^- \rightarrow \nu \bar{\nu} \gamma$$





extra dim.

$n = 4$

3

2



higher  $\mathcal{L}$  (1000  $\text{fb}^{-1}$ )

higher  $\sqrt{s}$  (800 GeV)

Polarisation

(5) G. Wilson

$\sqrt{s} = 800 \text{ GeV} \quad \mathcal{L} = 1 \text{ ab}^{-1}$

# ULTIMATE REACH

Example:  $d=2$ ,  $M_D$  sensitivity.

No  $\beta$   $P_{e^-} = 0.8$   $(P_-, P_+) = (0.8, 0.6)$

6.2 TeV	7.6 TeV	9.3 TeV
0.4%	1.0%	1.5%
5.7	2.6	1.7
1320	270	113
7.8 TeV	9.5 TeV	11.7 TeV

$5\sigma$   
(statistical)

$S/B$   $15\sigma$

$\sigma_S$  (fb)

$\sigma_b$  (fb)

95% CL  
limit

Systematics:  $\theta$  (1%) experimental  $\rightarrow$  "less polarised" limit potential.

Theory errors for  $\frac{\Delta L}{L}$  and  $\sigma_{\text{jet}}$  a major concern.

sensitivity at LHC (J. Hewett): 4.5 TeV for  $n=2$

$\gamma\gamma \rightarrow WW$

T. RIZZO

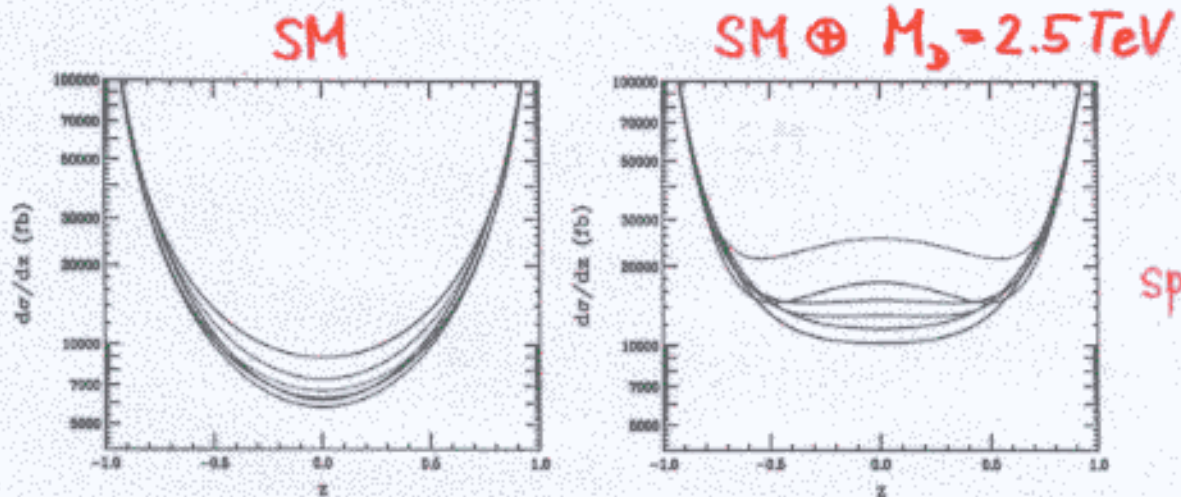


Fig. 3. Differential cross section for  $\gamma\gamma \rightarrow W^+W^-$  at a 1 TeV  $e^+e^-$  collider for (left) the SM and with  $M_H = 2.5$  TeV with (right)  $\lambda = 1$ . The  $\lambda = -1$  results are quite similar. In (left) from top to bottom in the center of the figure the helicities are  $(++++)$ ,  $(+++ -)$ ,  $(- + + -)$ ,  $(+ + - -)$ ,  $(+ - - -)$ , and  $(+ - + -)$ ; in (right) they are  $(- + + -)$ ,  $(+ - + -)$ ,  $(+ + + -)$ ,  $(+ - - -)$ ,  $(+ + + +)$ , and  $(+ + - -)$ , where we have employed the notation  $(P_{e1}, P_{l1}, P_{e2}, P_{l2})$ .



$\gamma\gamma \rightarrow WW$

T. RIZZO

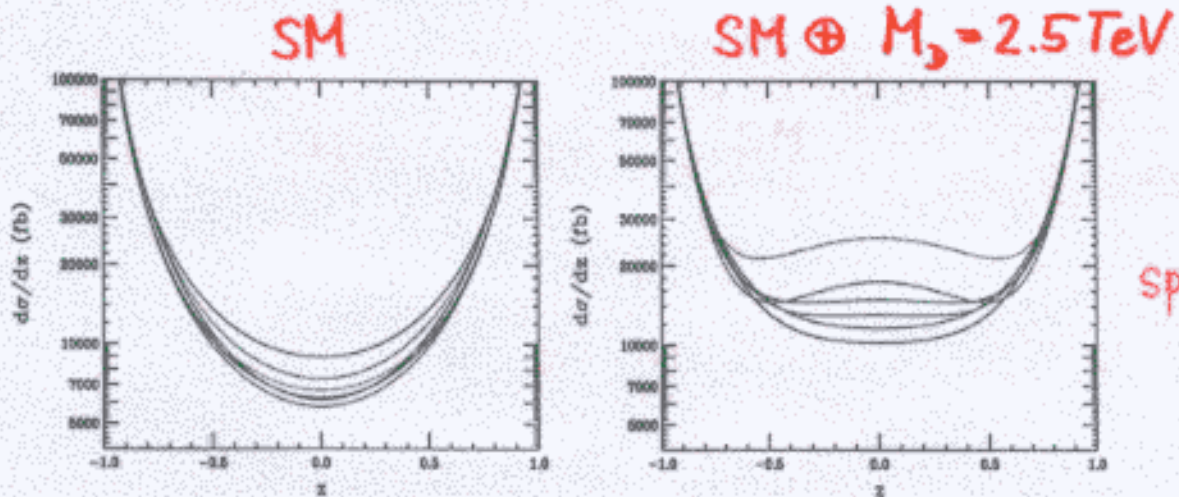


Fig. 3. Differential cross section for  $\gamma\gamma \rightarrow W^+W^-$  at a 1 TeV  $e^+e^-$  collider for (left) the SM and with  $M_H = 2.5$  TeV with (right)  $\lambda = 1$ . The  $\lambda = -1$  results are quite similar. In (left) from top to bottom in the center of the figure the helicities are  $(++++)$ ,  $(+++-)$ ,  $(-+-)$ ,  $(++--)$ ,  $(+---)$ , and  $(+-+-)$ ; in (right) they are  $(-+-)$ ,  $(+-+-)$ ,  $(++++)$ ,  $(+---)$ ,  $(++++)$ , and  $(++--)$ , where we have employed the notation  $(P_{e1}, P_{l1}, P_{e2}, P_{l2})$ .

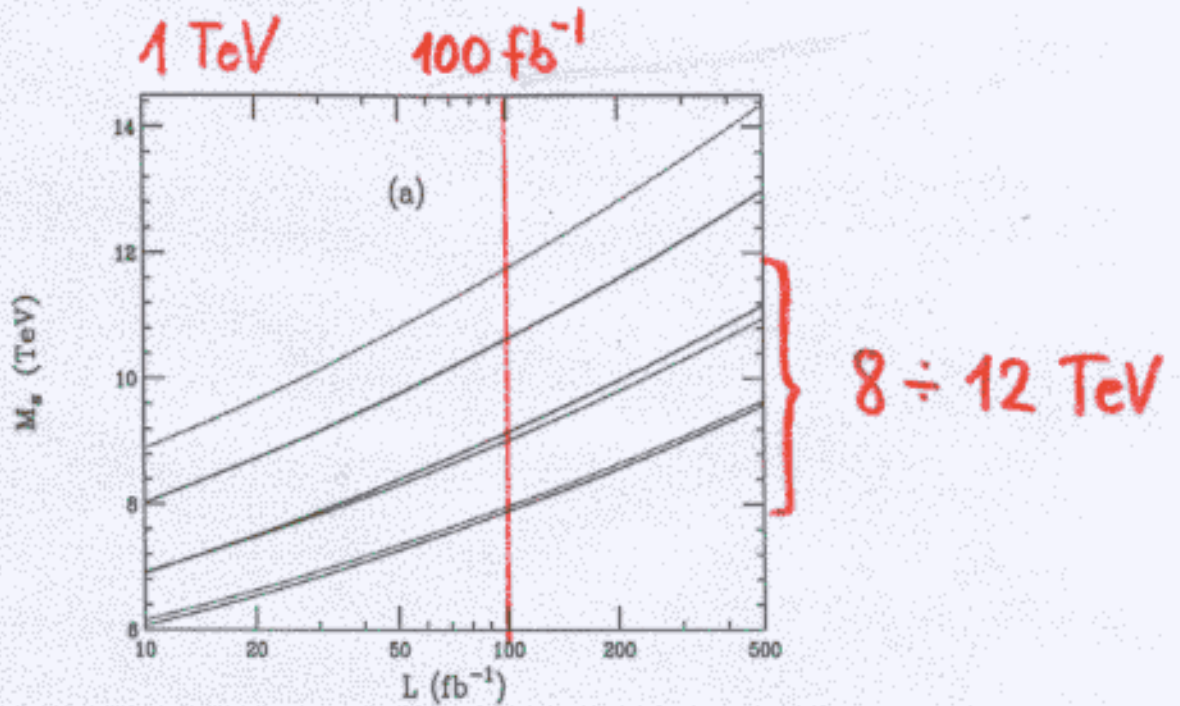


Fig. 6.  $M_H$  discovery reach for the process  $\gamma\gamma \rightarrow W^+W^-$  at a 1 TeV  $e^+e^-$  collider as a function of the integrated luminosity for the different initial state polarizations assuming  $\lambda = 1$ . From top to bottom on the right hand side of the figure the polarizations are  $(- + +-)$ ,  $(+ - --)$ ,  $(+ + --)$ ,  $(+ - +-)$ ,  $(+ - --)$ , and  $(+ + ++)$ .

# → HIGGS MECHANISM

## The stealthy Higgs model. van der Bij

In the presence of extra singlet scalars a large invisible width of the Higgs boson is possible. Such a Higgs boson is undetectable at the LHC. It can be studied at TESLA in the process  $e^+e^- \rightarrow ZH$ , where the Higgs boson is seen as missing energy. A completely clean signal exists in the leptonic channel. The lagrangian density is given by [1]:

$$\mathcal{L} = -\partial_\mu \phi^+ \partial^\mu \phi - \lambda(\phi^+ \phi - v^2/2)^2 - 1/2 \partial_\mu \vec{\varphi} \partial^\mu \vec{\varphi} - 1/2 m^2 \vec{\varphi}^2 - \kappa/(8N) (\vec{\varphi}^2)^2 - \omega/(2\sqrt{N}) \vec{\varphi}^2 \phi^+ \phi$$

The extra singlets can play a role as dark matter, in technicolor scenarios or in higher dimensions. From Fig. 1 we conclude, that TESLA can cover the allowed parameter range up to the kinematic limit and could therefore discover the Higgs boson if unseen at the LHC.

will be extended

## References

[1] T. Binoth, J. J. van der Bij, *Z. Phys. C* 75, 17 (1997) and references therein.

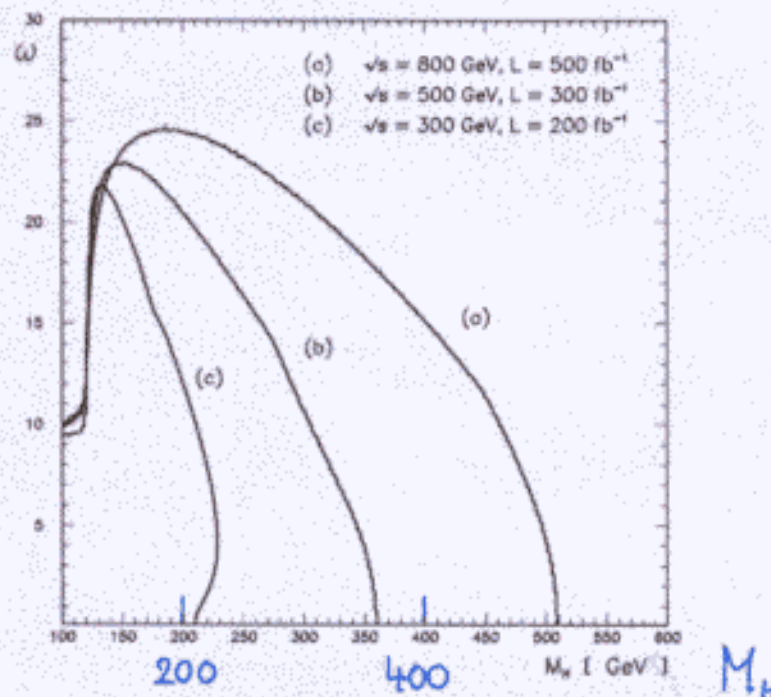
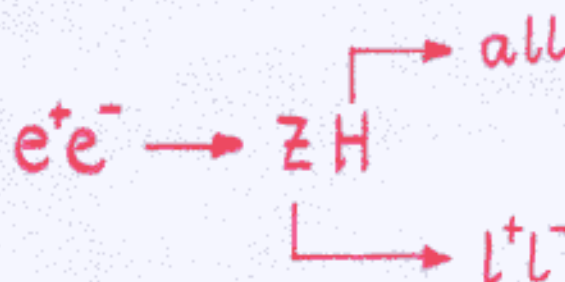
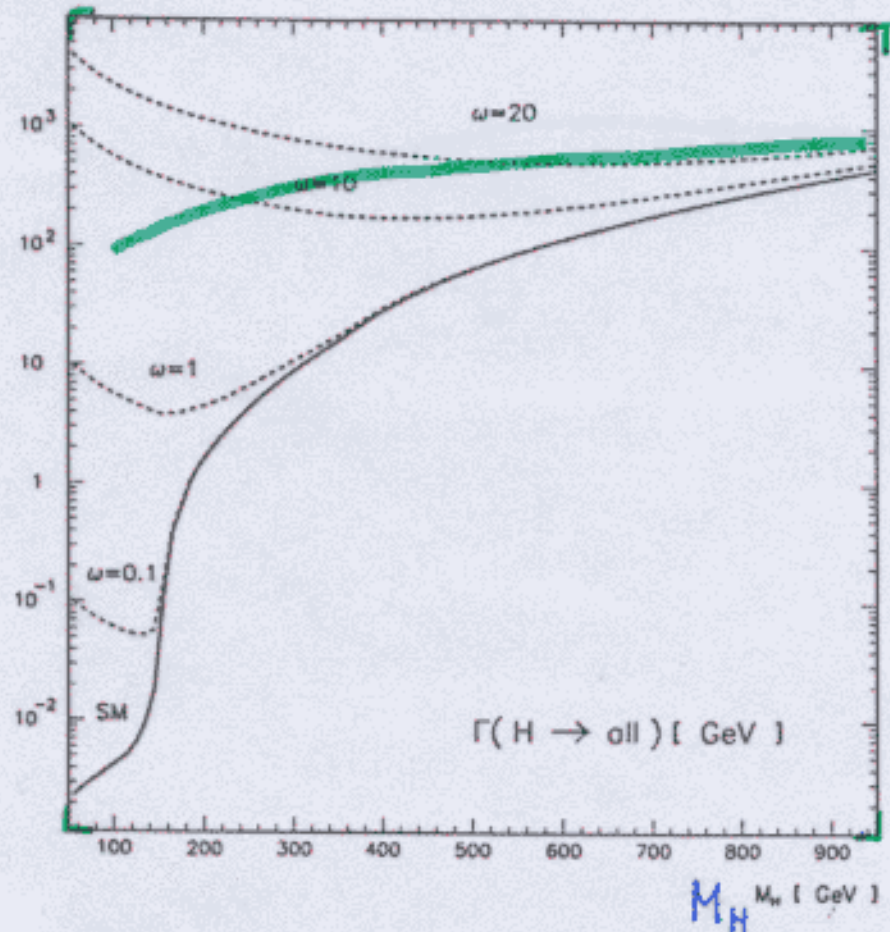
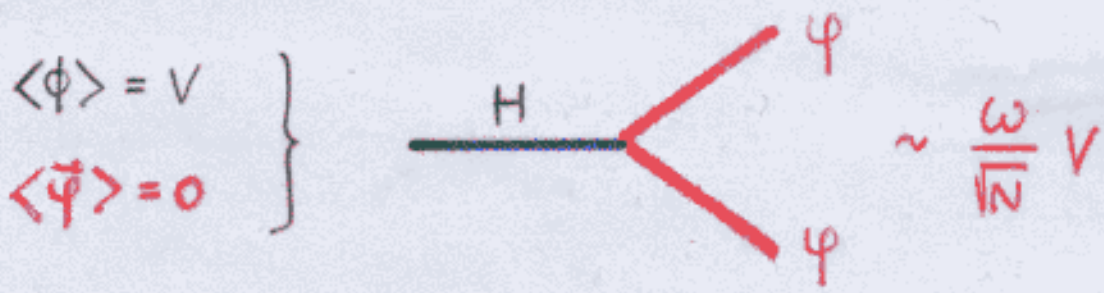


Figure 1: Exclusion limits on the parameters of the model in the  $\omega$  vs.  $M_H$  plane.





$\Gamma_H / M_H = 1$

Fig. to be added

Figure 1: Higgs width in comparison with the Standard Model.

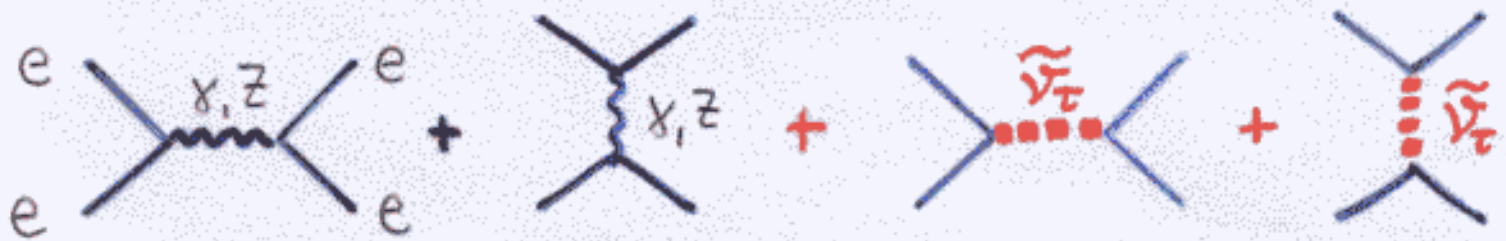
Phion mass the bounds can be found by rescaling the decay widths (appropriate phase space factor.)

ads

collider (LC) the upper limits on the couplings in the present model (mostly from the invisible decay, as the branching ratio into visible particles increases with increasing  $\varphi$ -Higgs coupling, whereas for the Higgs mass limits one has also visible decays, too. The  $WW$ -fusion process can not be used to look for  $\varphi$  decay. One is therefore left with the Higgsstrahlung und  $ZZ$ -fusion processes. At energies up to 500 GeV the Higgsstrahlung cross section is dominant and comparable if one multiplies with the branching ratio  $B(Z \rightarrow e^+e^-, \mu^+\mu^-)$ . The  $ZZ$ -fusion reaction is preferred, because one can tag the on-shell Z boson. We have considered reactions containing an on shell Z boson with its decay into  $e^+e^-$  or  $\mu^+\mu^-$ . The signal cross section is the well known Higgsstrahlung cross section multiplied by the non standard Higgs width due to Phion decay. With the

→ SUSY:  $\mathcal{R}$

Bhabha Scattering  $e^+e^- \rightarrow \tilde{\nu}_\tau \rightarrow e^+e^-$  Rückl



at resonance

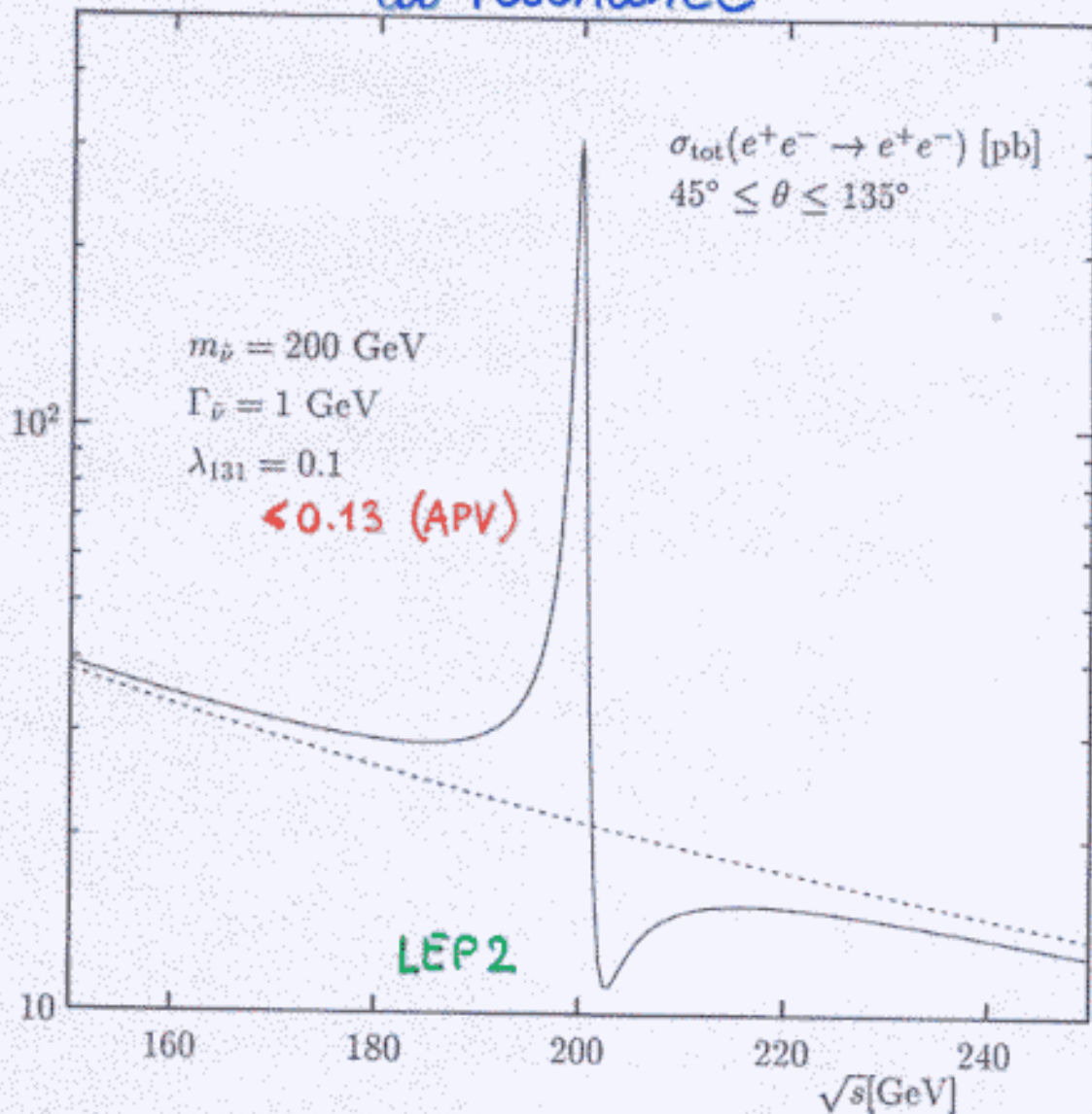


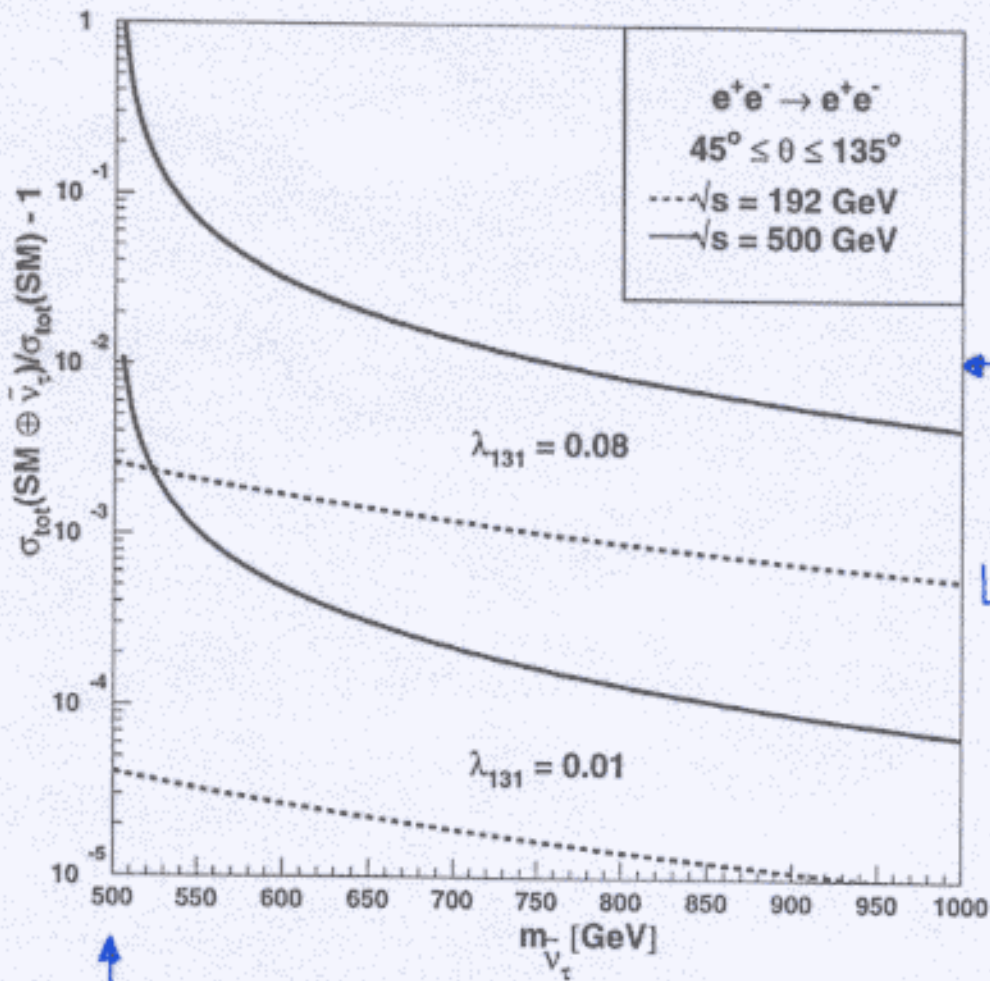
Figure 5: Cross section for Bhabha scattering including  $\tilde{\nu}_\tau, \bar{\tilde{\nu}}_\tau$  sneutrino resonance formation for  $45^\circ \leq \theta \leq 135^\circ$  as a function of the  $e^+e^-$  center-of-mass energy. Parameters:  $m_{\tilde{\nu}} = 200 \text{ GeV}$ ,  $\Gamma_{\tilde{\nu}} = 1 \text{ GeV}$ , and  $\lambda_{131} = 0.1$ .

Kalinowski et al.

extrapolation to  $m_{\tilde{g}} = 650 \text{ GeV}$

$\sqrt{s} = 500 - 800 \text{ GeV}$

off resonance



← 1% effect

LEP2

↑ resonance

## Resonant single chargino production

Lola

An alternative possibility to resonant Bhabha scattering, is resonant single chargino or neutralino production<sup>1</sup> [1]. Which final state will dominate, clearly depends on (i) the SUSY parameter space and (ii) the strength of the R-violating Yukawa coupling  $\lambda$ . This is shown in Figure 1, where (assuming the gaugino unification relation  $M_1 = (5/3) \tan^2 \theta_W M_2$ ), we present contour plots for the branching ratio for the  $\tilde{\nu}$  decay to fermions.

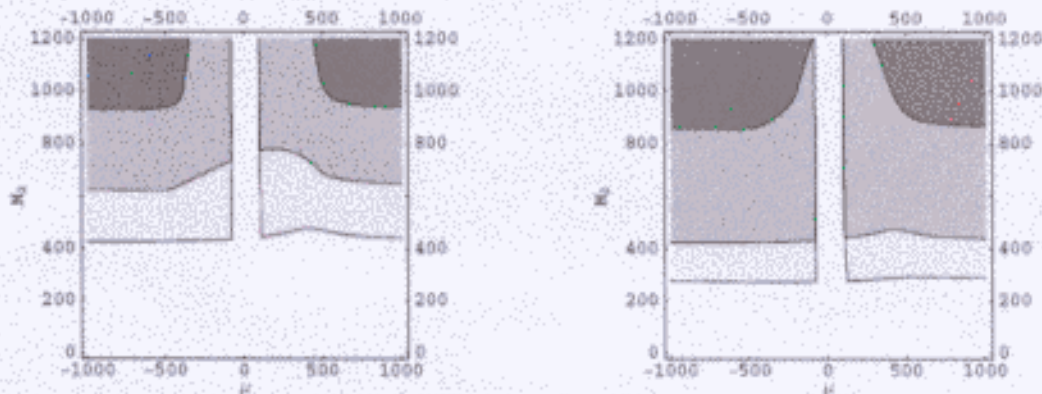


Figure 12:  $B$  for  $\tilde{\nu}$  decay to fermions for parameters of interest for the LC. We present contours for  $B \geq 0.9, 0.3, 0.1$ , from the darker to the lighter areas respectively. We choose  $\tan\beta = 2.0, m_{\tilde{\nu}} = 500 \text{ GeV}$  and  $\lambda = 0.1$  (left) and  $0.2$  (right). The LEP2 bound on charginos has been implemented.

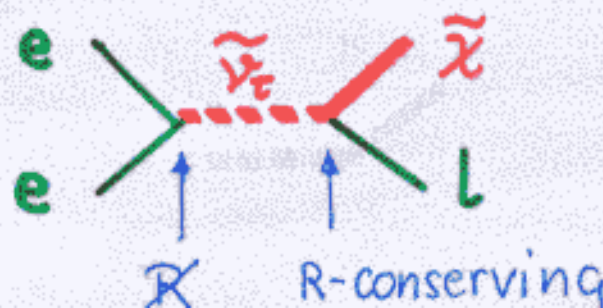
For large  $M_2, \mu$ , resonant Bhabha scattering is the most significant channel. However, for smaller  $M_2, \mu$ , which occurs for a wide part of the parameter space relevant for the LC, chargino and neutralino final states dominate. It actually turns out that there exist bands of the parameter space where the production of even the heavier charginos and neutralinos may occur at a significant level. This is shown in Table 2, where we present the decay widths for the production of each chargino and neutralino separately.

Once single charginos and neutralinos have been produced, we may expect chains of cascade decays to SM fermions with striking events, such as like-sign lepton signals (due to the Majorana nature of the neutralinos). It is therefore important to include single chargino and neutralino productions among the search channels for supersymmetry at the LC.

## References

- [1] S. Lola, LC-TH-1999-021, hep-ph/9912217

<sup>1</sup> $W$ -slepton and  $Z$ -sneutrino productions are comparatively suppressed for a relatively heavy slepton spectrum, especially close to the resonance.



scenarios with  $\text{Br}(\tilde{\chi}L) > \text{Br}(e^+e^-)$

$M_2$	$\mu$	$\Gamma_1$	$\Gamma_2$	$\Gamma_3$	$\Gamma_4$	$\Gamma'_1$	$\Gamma'_2$
200.	200.	1.09	0.28	0.01	0.58	2.09	0.88
200.	600.	0.72	1.38	–	–	3.06	–
300.	200.	0.82	0.01	0.01	0.50	0.92	0.87
300.	600.	0.62	0.85	–	–	1.88	–
400.	200.	0.53	0.01	0.05	0.15	0.42	0.27
400.	600.	0.51	0.33	–	–	0.74	–
500.	200.	0.31	–	0.14	–	0.23	–
500.	600.	0.41	0.03	–	–	0.08	–

Table 4: All units in the table are in GeV.  $\Gamma_i$  are the decay rates for the four neutralinos, while  $\Gamma'_i$  the decay rates for the two charginos. We chose  $\tan\beta = 2$ ,  $\lambda = 0.1$  and  $m_{\tilde{g}} = 500$  GeV. For this choice of parameters, the R-violating decay rate is 0.1 GeV.



$$e^+e^- \rightarrow \tilde{\nu} \rightarrow \tilde{\chi} l$$

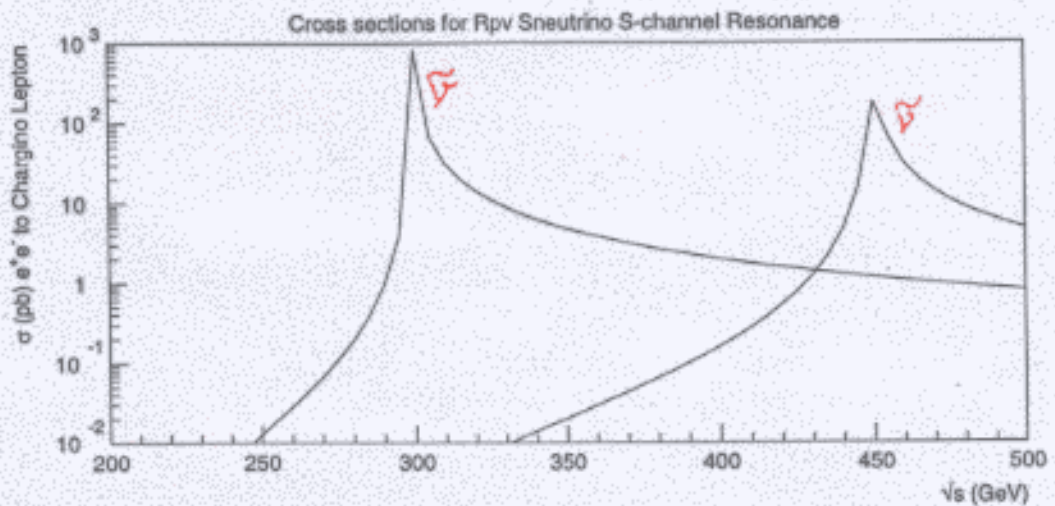
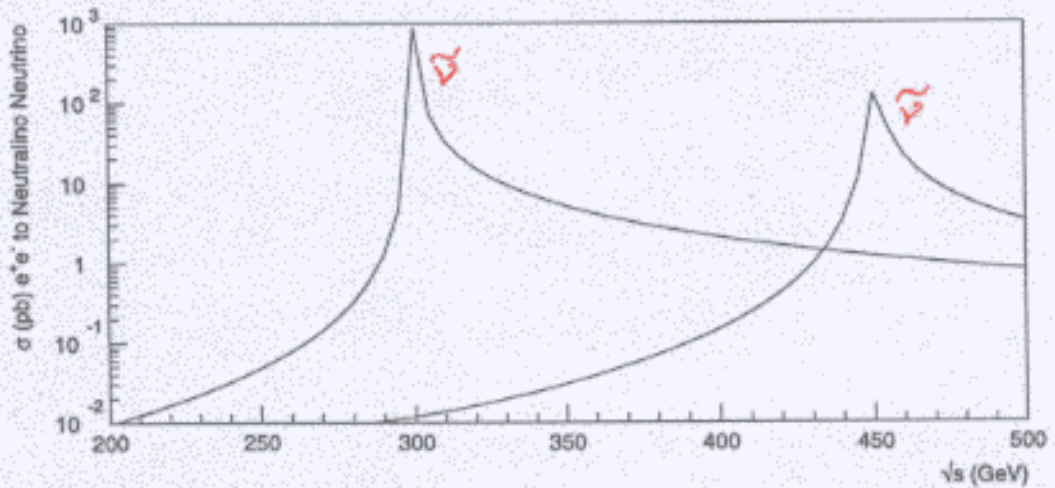
 $\tilde{\chi}^\pm$ 

 $\tilde{\chi}^0$ 


Figure 3: Cross sections for single chargino and neutralino productions, including effects from initial state radiation (ISR), for two different sneutrino masses. The parameters we choose for this plot are the following:  $m_{\tilde{\nu}} = 300$  and  $450$  GeV respectively;  $m_{\tilde{Z}} = 1000$  GeV;  $\tan\beta = 2$ ,  $\lambda = 0.1$ ,  $\mu = -200$  GeV,  $M_2 = 250$  GeV. In this case, all charginos and neutralinos are produced.

# → HIGH PRECISION PHYSICS : GigaZ

Illana Riemann

## 3.1.1 Rare Z decays, Lepton Flavor Violation in Z decays

If a process is forbidden in Born approximation in the Standard Model SM, as e.g. *lepton flavor violation* (LFV), a small rate could be nevertheless expected through virtual corrections, of order:

$$\text{BR} \sim (\alpha/\pi)^2 \approx 5 \times 10^{-6}. \quad (10)$$

With the GigaZ option one may expect the production of about  $10^9$  Z bosons at resonance, about a factor 100 higher than at LEP 1. Thus, GigaZ will become sensitive to a whole class of rare decays of the Z (or of secondary particles like the  $\tau$  lepton), even if some small factors like mixing angles might appear.

As examples we use the decays  $Z \rightarrow e\mu, \mu\tau, e\tau$  [1]. The best direct limits were obtained at LEP 1, e.g. :  $\text{BR}(Z \rightarrow \mu^\mp \tau^\pm) < 1.2 \times 10^{-5}$  (95% c.l.) [2]. They could be largely improved at GigaZ [3]:

$$\text{BR}(Z \rightarrow \mu^\mp \tau^\pm) = \frac{\Gamma(Z \rightarrow \mu^+ \tau^- + \mu^- \tau^+)}{\Gamma_Z} \leq 10^{-8}, \quad (11)$$

and LFV Z decays might get observable.

There are several quite different potential sources of LFV Z decays:

**a) Heavy neutrinos.** After the evidences for neutrino masses and mixings from astrophysics, one may quest for heavy, mixing partners of them, which then, in turn, could mediate LFV Z decays via loops. Figure 6 shows predictions from the  $\nu$ SM, the SM extended with massive and flavor mixing Dirac or Majorana neutrinos, with branching ratios up to  $\text{BR}(Z \rightarrow \mu^\mp \tau^\pm) = 10^{-7} \dots 10^{-5}$  [1]. Limits on the masses from unitarity and on the mixings from experiment are taken into account. Massive right-handed neutrinos appear also naturally in left-right symmetric models, with similar branching ratios [4].

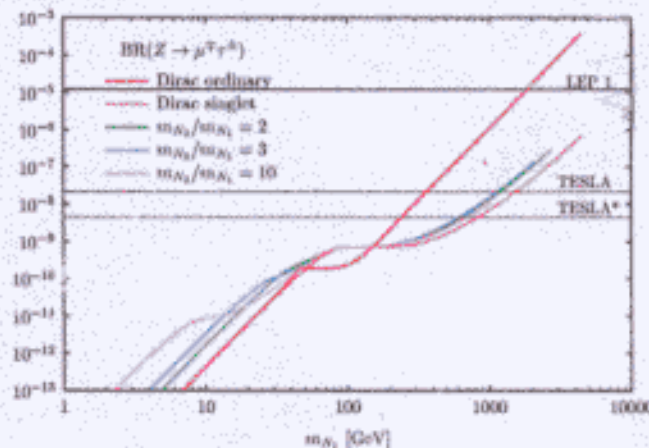
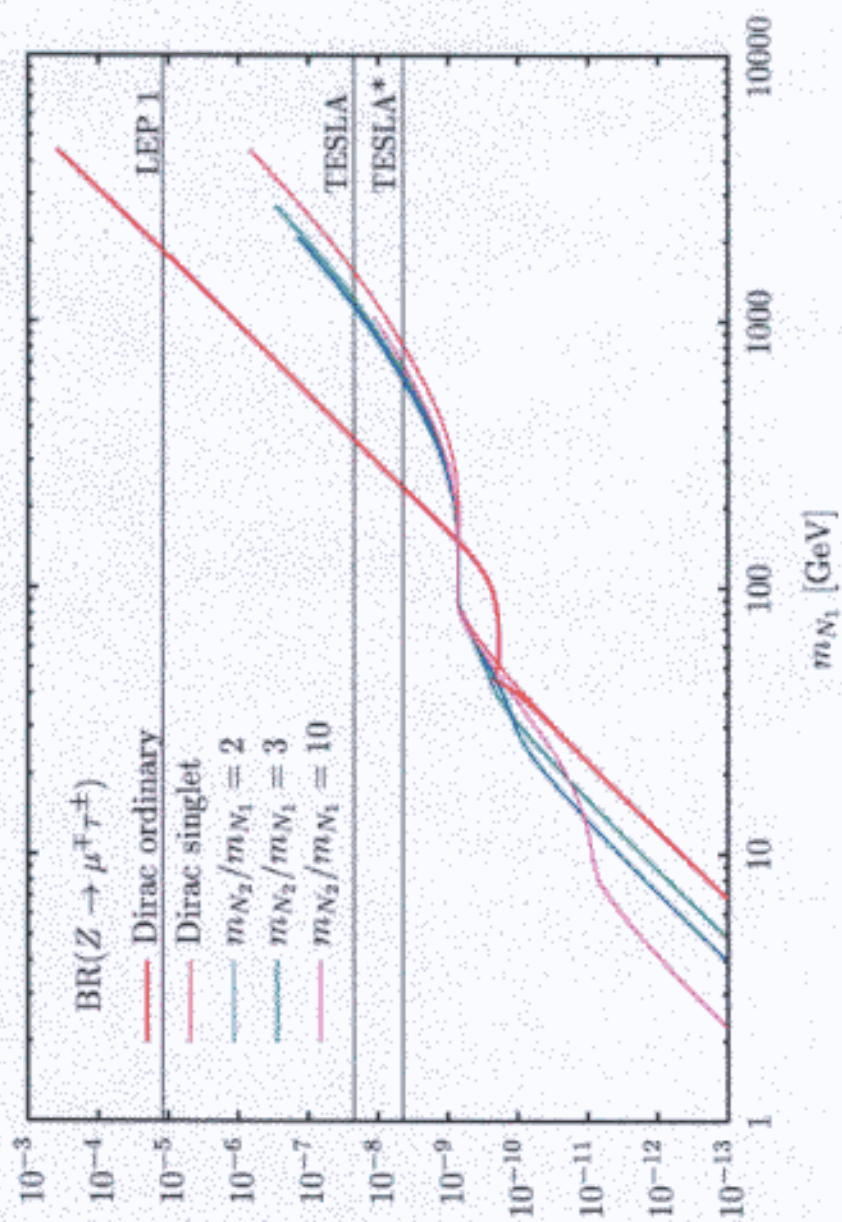


Figure 6: Upper limit for  $\text{BR}(Z \rightarrow \mu^\mp \tau^\pm)$  if the SM is extended with: (i) one heavy ordinary (thick solid) or singlet (thin solid) Dirac neutrino of mass  $m_{N_1}$ ; (ii) two heavy right-handed singlet Majorana neutrinos (dashed lines) with masses  $m_{N_1}$  and  $m_{N_2}$ .

add comment on constraints from  $\mu \rightarrow e\gamma, eee$



b) Leptoquarks. Many extensions of the SM predict leptoquarks: string-inspired models, technicolour, composite models, left-right symmetric models, non-minimal supersymmetric models with broken  $R$  parity, and even the strongly coupled version of the SM. They might also contribute in higher orders. The branching ratio is then proportional to at least one generation non-diagonal Yukawa coupling of the leptoquarks [5]:  $\text{BR}(Z \rightarrow \mu^\mp \tau^\pm) \lesssim 10^{-9}$ .

c) Heavy neutral gauge bosons  $Z'$ . A heavy  $Z'$ , with family non-universal couplings to fermions and mixing with the  $Z$  boson, induces non-diagonal couplings of the  $Z$  to fermions at tree-level [6]. Taking present bounds on couplings and on the mass of a  $Z'$ , one gets  $\text{BR}(Z \rightarrow \mu\tau) \lesssim 10^{-11}$ .

d) Supersymmetry. In supersymmetric theories with unbroken  $R$  parity, the LFV  $Z$  decays may proceed via loops with virtual sleptons with intergeneration mixing. The bounds on hadronic FCNC phenomena constrain the amount of slepton mixing and hence the LFV  $Z$  decays to [7]:  $\text{BR}(Z \rightarrow \ell_1 \ell_2) \lesssim 10^{-7}$ . Even more promising are the *left-right supersymmetric models*, mainly due to the contribution of the fermionic superpartner of the doubly charged Higgs boson,  $\tilde{\Delta}_R^{\pm\pm}$  [8], although  $\mu \rightarrow e\gamma$  constrains the LR SUSY parameter space.

The supersymmetric theories are perhaps most promising and deserve more attention. In sum, we see a potential of GigaZ for a study of LFV  $Z$  decays. This result encourages further investigation.

will be dropped

## References

- [1] J. I. Illana et al., LC-TH-2000-007, hep-ph/0001273; *Nucl. Phys. B Proc. Suppl.* **89** (2000) 64.
- [2] Particle Data Group, C. Caso et al., *Eur. Phys. J. C* **3** (1998) 1.
- [3] G. Wilson, talks at DESY-ECFA LC Workshops, Frascati (1998) and Oxford (1999).
- [4] A. Pilaftsis, *Phys. Rev.* **D52** (1995) 459.
- [5] M. A. Doncheski et al., *Phys. Rev.* **D40** (1989) 2301.
- [6] P. Langacker and M. Plümacher, *Phys. Rev.* **D62** (2000) 013006.
- [7] M. J. Levine, *Phys. Rev.* **D36** (1987) 1329; F. Gabbiani et al., *Phys. Lett.* **B214** (1988) 398.
- [8] M. Frank and H. Hamidian, *Phys. Rev.* **D54** (1996) 6790.

# → HIGH PRECISION PHYSICS

## 3.2.1 Extended Gauge Theories

Riemann S.

In grand unified theories the unified symmetry group must be broken at the unification scale  $\Lambda_{\text{GUT}} \gtrsim 10^{16}$  GeV in order to be compatible with the experimental bounds on the proton lifetime. However, the breaking to the SM group may occur in several steps and some subgroups may remain unbroken down to a scale of order 1 TeV. In this case the surviving group factors allow for *new gauge bosons* with masses not far above the scale of electroweak symmetry breaking. Besides SU(5), two other unification groups have received much attention: In SO(10) three new gauge bosons  $W_R^\pm, Z_R$  may exist, in  $E_6$  a light neutral  $Z'$  in the TeV range.

expand

The virtual effects of a new  $Z'$  or  $Z_R$  vector boson associated with the most general effective theories which arise from breaking  $E(6) \rightarrow SU(3) \times SU(2) \times U(1) \times U(1)_{Y'}$  and  $SO(10) \rightarrow SU(3) \times SU(2)_L \times SU(2)_R \times U(1)$ , have been investigated [1]. Assuming that the  $Z'$  ( $Z_R$ ) are heavier than the available c.m. energy, the propagator effects on various observables of the process

$$e^+e^- \xrightarrow{\gamma, Z, Z'} f\bar{f}$$

have been studied.

Here, the sensitivity reach to detect  $Z'$  bosons is studied for three center-of-mass energies ( $\sqrt{s} = 500$  GeV, 800 GeV, 1 TeV) and for different scenarios of accuracy:

• case A:

$$\Delta P_{e^\pm} = 1.0\%, \Delta \mathcal{L} = 0.5\%, \Delta^{\text{sys}} \epsilon_{\text{lepton}} = 0.5\%, \Delta^{\text{sys}} \epsilon_{\text{hadron}} = 0.5\%;$$

• case B:

$$\Delta P_{e^\pm} = 0.5\%, \Delta \mathcal{L} = 0.5\%, \Delta^{\text{sys}} \epsilon_{\text{lepton}} = 0.5\%, \Delta^{\text{sys}} \epsilon_{\text{hadron}} = 0.5\%;$$

• case C:

$$\Delta P_{e^\pm} = 0.5\%, \Delta \mathcal{L} = 0.2\%, \Delta^{\text{sys}} \epsilon_{\text{lepton}} = 0.3\%, \Delta^{\text{sys}} \epsilon_{\text{hadron}} = 0.5\%;$$

• case D: **0.5%**

$$\Delta P_{e^\pm} = 0.1\%, \Delta \mathcal{L} = 0.2\%, \Delta^{\text{sys}} \epsilon_{\text{lepton}} = 0.1\%, \Delta^{\text{sys}} \epsilon_{\text{hadron}} = 0.1\%;$$

relative errors !

drop

An integrated luminosity of  $1000 \text{ fb}^{-1}$  is assumed to be collected at each centre-of-mass energy. The polarization of electrons and positrons are 80% and 60%, respectively. The corresponding lower bounds (95% CL) on the  $Z'$  masses are given in Table 2. Below a  $Z'$  resonance measurements of fermion-pair production are sensitive only to the ratio of  $Z'$  couplings and  $Z'$  mass. If a  $Z'$  will be detected at LHC its origin can be found by determining the  $Z'$  couplings. Figure 9 demonstrates the resolution power between  $Z'$  models assuming that the mass of the new boson is measured at LHC. Here, leptonic final states are considered and lepton-universality is supposed. If the potential  $Z'$  is heavier than 4.5 TeV and/or it does not couple to quarks, there will be no sensitivity to  $m_{Z'}$  at LHC. Nevertheless, the analysis

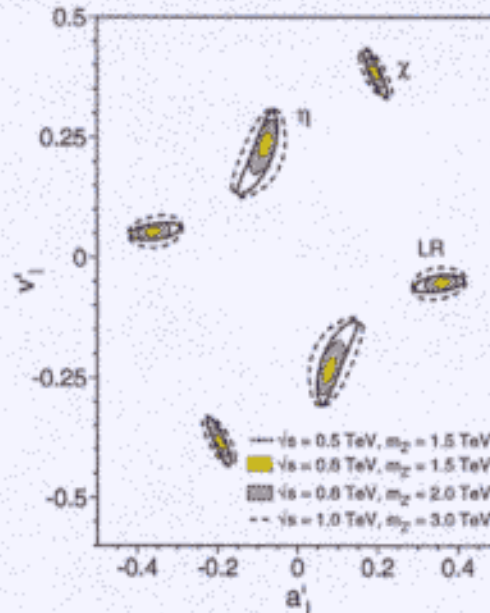
also  $P_{e^\pm} = 0$

$\sqrt{s}[\text{TeV}]$	errors	$\chi$	$\psi$	$\eta$	LR
0.5	A	6290	2190	3300	7530
<del>0.5</del>	<del>B</del>	<del>6320</del>	<del>2340</del>	<del>3520</del>	<del>9540</del>
<del>0.5</del>	<del>C</del>	<del>6620</del>	<del>2740</del>	<del>3730</del>	<del>9570</del>
0.5	D	7260	3590	4290	11570
0.8	A	8350	3400	4570	11790
<del>0.8</del>	<del>B</del>	<del>8410</del>	<del>3520</del>	<del>4770</del>	<del>13620</del>
<del>0.8</del>	<del>C</del>	<del>9090</del>	<del>4080</del>	<del>5210</del>	<del>13670</del>
0.8	D	10150	4860	5960	14830
1.0	A	9680	4160	5340	14270
<del>1.0</del>	<del>B</del>	<del>9760</del>	<del>4240</del>	<del>5520</del>	<del>15780</del>
<del>1.0</del>	<del>C</del>	<del>10700</del>	<del>4870</del>	<del>6130</del>	<del>15850</del>
1.0	D	11960	5595	7000	16710

⇒ Plot



Table 2: Sensitivity to lower bounds on the  $Z'$ ,  $Z_R$  masses (95% C.L.) in  $E_6$  ( $\chi$ ,  $\psi$  and  $\eta$  realization) and left-right symmetric models;  $m_{Z'}$ ,  $m_{Z_R}$  are given in GeV. The integrated luminosity is  $1000 \text{ fb}^{-1}$ ; the error scenarios A – D are described in the text.



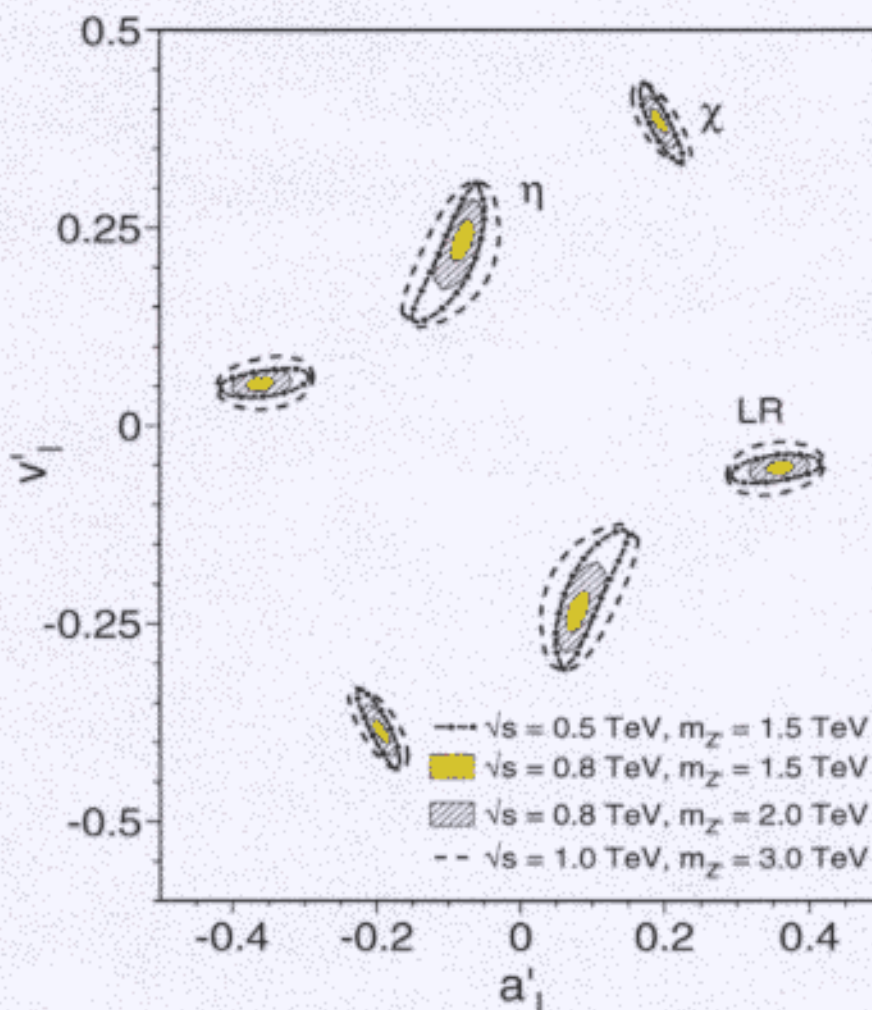
sign ambiguity

Figure 9: Resolution power for different  $m_{Z'}$  (95% CL) based on measurements of leptonic observables at  $\sqrt{s}=500 \text{ GeV}$ ,  $800 \text{ GeV}$ ,  $1 \text{ TeV}$  with a luminosity  $\mathcal{L}_{int} = 1000 \text{ fb}^{-1}$ . The leptonic couplings of the  $Z'$  correspond to the  $\chi$ ,  $\eta$  or LR model.

## Z' couplings to leptons

$$e^+ e^- \rightarrow l^+ l^-$$

- lepton universality
- $m_{Z'}$  is known from LHC:  $m_{Z'} \leq 4$  TeV
- $\Delta P_{e^\pm} = 0.5\%$ ,  $\Delta \mathcal{L} = 0.5\%$ ,  
 $\Delta^{sys} \epsilon_{lepton} = 0.5\%$ ,
- $\mathcal{L}_{int} = 1000 \text{ fb}^{-1}$



of fermion-pair production could detect a  $Z'$  and resolve the model. Instead of extracting the  $Z'$  couplings to fermions,  $v'_f, a'_f$ , normalized  $Z'$  couplings,  $a_f^N, v_f^N$ , have to be obtained:

$$a_f^N = a'_f \sqrt{\frac{s}{m_{Z'}^2 - s}}; \quad v_f^N = v'_f \sqrt{\frac{s}{m_{Z'}^2 - s}}. \quad (16)$$

Assuming a  $Z'$  with  $m_{Z'}=5$  TeV, its detection and identification will be possible as demon-

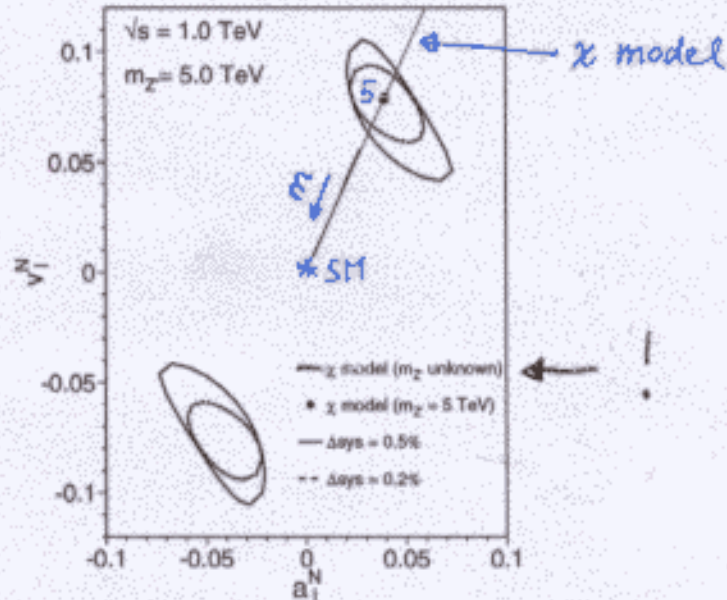


Figure 10: Resolution power (95% CL) for a  $Z'$  based on measurements of leptonic observables at  $\sqrt{s} = 1$  TeV and  $\mathcal{L}_{int} = 1000$  fb $^{-1}$ . The  $Z'$  is realized in the  $\chi$  model with  $m_{Z'}=5$  TeV; the  $Z'$  mass is unknown.

strated in Figure 10. A  $Z'$  is postulated with  $m_{Z'}=5$  TeV and with leptonic couplings as suggested in the  $\chi$  model. Measurements at  $\sqrt{s}=1$  TeV with  $\mathcal{L}=1000$  fb $^{-1}$  and accuracies of  $\Delta P_{e\pm} = 0.5\%$ ,  $\Delta\mathcal{L}=0.5\%$  and  $\Delta^{sys}\epsilon_{lepton}=0.5\%$  will allow to derive bounds on  $a_f^N, v_f^N$  as shown by the solid line. If  $\Delta^{sys}\epsilon_{lepton}=0.2\%$  and  $\Delta\mathcal{L}=0.2\%$  these bounds could be shrunk to the dashed-dotted line. On the line of the  $\chi$  model the allowed area in the  $(a_f^N, v_f^N)$ -plane is located around the point  $(a_f^N(m_{Z'} = 5 \text{ TeV}), v_f^N(m_{Z'} = 5 \text{ TeV}))$ . Fixing the leptonic  $Z'$  couplings to the  $\chi$  model, a mass range of  $4.3 \text{ TeV} \leq m_{Z'} \leq 6.2 \text{ TeV}$  is derived for  $\Delta sys = 0.5\%$  and  $4.5 \text{ TeV} \leq m_{Z'} \leq 5.9 \text{ TeV}$  for  $\Delta sys = 0.2$ , respectively.

It should be noted that a two-fold ambiguity in the signs of couplings remains since all observables are bilinear products of  $a'_f$  and  $v'_f$ .

## References

- [1] A. Djouadi, A. Leike, T. Riemann, D. Schaile and C. Verzegnassi, Z. Phys. C56 (1992) 289.

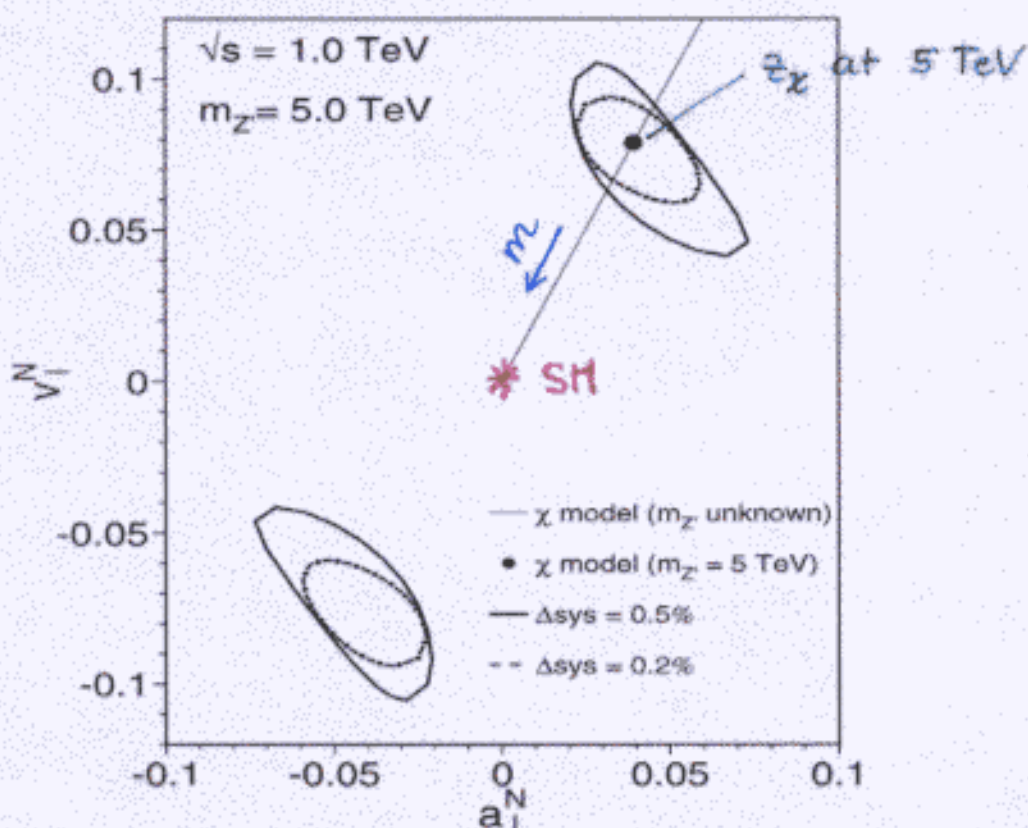


## Z' couplings to leptons

$$m_{Z'} > 4.5 \text{ TeV}$$

$$a_f^N = a'_f \sqrt{\frac{s}{m_{Z'}^2 - s}}; \quad v_f^N = v'_f \sqrt{\frac{s}{m_{Z'}^2 - s}}$$

- $\sqrt{s} = 1 \text{ TeV}$
- $\Delta P_{e^\pm} = 0.5\%$ ,  $\Delta \mathcal{L} = 0.5\%$ ,  
 $\Delta^{\text{sys}} \epsilon_{\text{lepton}} = 0.5\%$ ,  $0.2\%$
- $\mathcal{L}_{\text{int}} = 1000 \text{ fb}^{-1}$



- (1) test hypothesis ( $\chi$ ) indep. of mass
- (2) constrain mass for given model

# → HIGH PRECISION PHYSICS: extended gauge sym

## 3.2.2 $W'$ limits

Leike et al.

The limits on extra charged gauge bosons shown here are based on the two reactions  $e^+e^- \rightarrow \nu\bar{\nu}\gamma$  and  $e\gamma \rightarrow \nu q + X$ . The SM inputs  $M_W = 80.33 \text{ GeV}$ ,  $M_Z = 91.187 \text{ GeV}$ ,  $\sin^2\theta_W = 0.23124$ ,  $\alpha = 1/128$  and  $\Gamma_Z = 2.49 \text{ GeV}$  are used in the numerics.

Details of the  $W'$  analysis based on  $e^+e^- \rightarrow \nu\bar{\nu}\gamma$  can be found in reference [1]. In order to take into account detector acceptance, the photon energy,  $E_\gamma$ , and the angle of the photon with respect to the beam axis,  $\theta_\gamma$ , are restricted to the ranges  $E_\gamma \geq 10 \text{ GeV}$  and  $10^\circ \leq \theta_\gamma \leq 170^\circ$ . These cuts also remove singularities arising for soft or collinear photons. The photon's transverse momentum is restricted to  $p_T^\gamma > \sqrt{s} \sin\theta_\gamma \sin\theta_v / (\sin\theta_\gamma + \sin\theta_v)$ , where  $\theta_v$  is the minimum angle down to which the veto detectors may observe electrons or positrons, here  $\theta_v = 25 \text{ mrad}$ . This cut removes the largest background, namely radiative Bhabha-scattering where the scattered  $e^+$  and  $e^-$  go undetected down the beam pipe.

Figure 1 shows the possible constraints (95% C.L.) on the right- and left-handed couplings of a  $W'$  to fermions using the total cross section  $\sigma$  and the left-right asymmetry  $A_{LR}$  as observables. The assumed systematic errors for  $\sigma(A_{LR})$  are 2%(1%), 80% electron and 60% positron polarization are assumed. It is assumed in this figure that there exists a heavy  $W'$  with couplings exactly as the SM  $W$ -Boson (SSM  $W'$ ) and that there is no signal from additional neutral gauge bosons. The systematic errors dominate the  $W'$  limits. The  $W'$  couplings can only be constrained up to a two-fold ambiguity. This ambiguity could be resolved by reactions where the  $W'$  couples to a triple gauge vertex.

Details of the  $W'$  analysis based on  $e\gamma \rightarrow \nu q + X$  can be found in reference [2]. In order to take into account detector acceptance, the angle  $\theta_q$  of the detected quark relative to the beam axis is restricted to  $10^\circ \leq \theta_q \leq 170^\circ$ . The quark's transverse momentum relative to the beam is restricted to  $p_T^q > 40(75) \text{ GeV}$  for  $\sqrt{s} = 0.5(1.0) \text{ TeV}$ . This cut suppresses various SM backgrounds.

Figure 2 shows possible constraints on the couplings of a  $W'$  to fermions for backscattered laser photons. The best  $W'$  limits come from the observable  $d\sigma/dp_T^q$ . As in  $e^+e^-$  scattering, the assumed systematic error of 2% dominates the statistical error, thus eliminating the potential gain from high luminosities.  $W'$  limits from backscattered laser photons are considerably better than those from Weizsäcker Williams photons. Polarized beams give only a minor improvement to  $W'$  limits after the inclusion of systematic errors. Shown are regions of  $W'$  couplings, which can be excluded, relative to the SM, with 95% confidence. Note the different normalization of the couplings in Figures 1 and 2;  $L_L(W') = C_L \cdot g / (2\sqrt{2})$  with a similar relation between  $R_L(W')$  and  $C_R$ .

The table shows mass discovery limits from both reactions for a  $W'$  predicted in various models. LRM means a  $W'$  predicted in the left-right model with  $\kappa = 1$  and  $\rho = 1$ . KK stands for the Kaluza-Klein-Model. All assumptions are the same as in figures 1 and 2. The  $e^+e^-$  limits on the SSM  $W'$  do not improve with polarized beams. The  $e^+e^-$  limits on the  $W'$  predicted in the LRM (KK) show a weak (considerable) improvement with polarized beams. As mentioned before, the  $e\gamma$  limits do not improve much with polarized beams. Backscattered

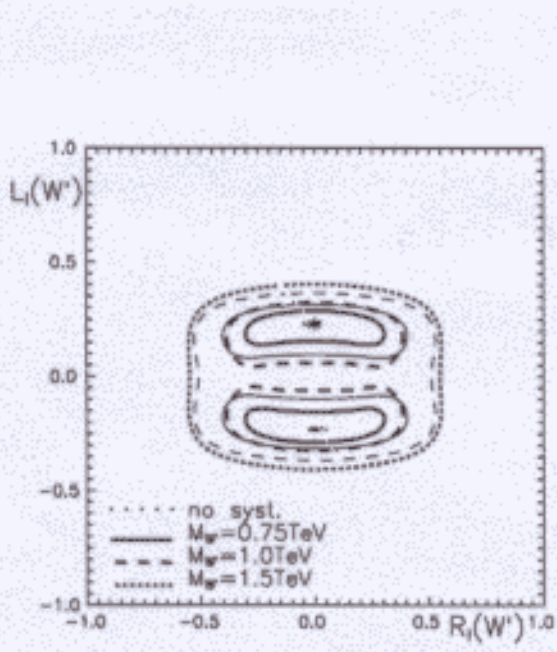


Figure 1: 95% C.L. constraints on  $W'$  couplings for  $\sqrt{s} = 0.5 \text{ TeV}$  (thin lines) and  $\sqrt{s} = 1.0 \text{ TeV}$  (thick lines) and  $L_{int} = 1000 \text{ fb}^{-1}$  with a systematic error for different  $W'$  masses. No systematic error is included for the dots. The couplings of the SSM  $W'$  are indicated by a star.

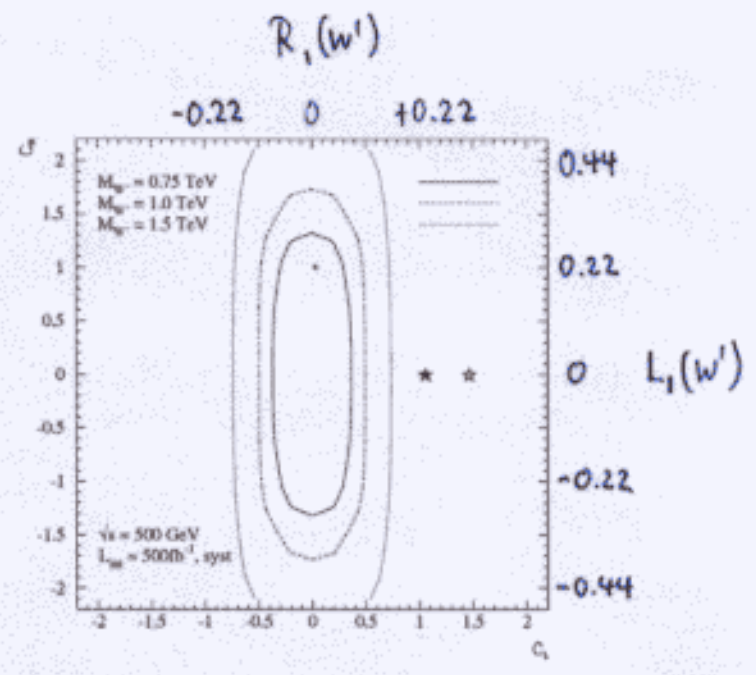


Figure 2: 95% C.L. constraints on  $W'$  couplings for  $\sqrt{s} = 0.5 \text{ TeV}$  and  $L_{int} = 500 \text{ fb}^{-1}$  with a 2% systematic error for different  $W'$  masses. The couplings corresponding to the SSM, LRM and the KK model are indicated by a full star, a dot and an open star, respectively.

laser photons give important complementary  $W'$  limits relative to  $e^+e^-$  scattering. See reference [1] for further details on  $W'$  limits from  $e^+e^-$  collisions and reference [2] for further details on  $W'$  limits from  $e\gamma$  collisions.

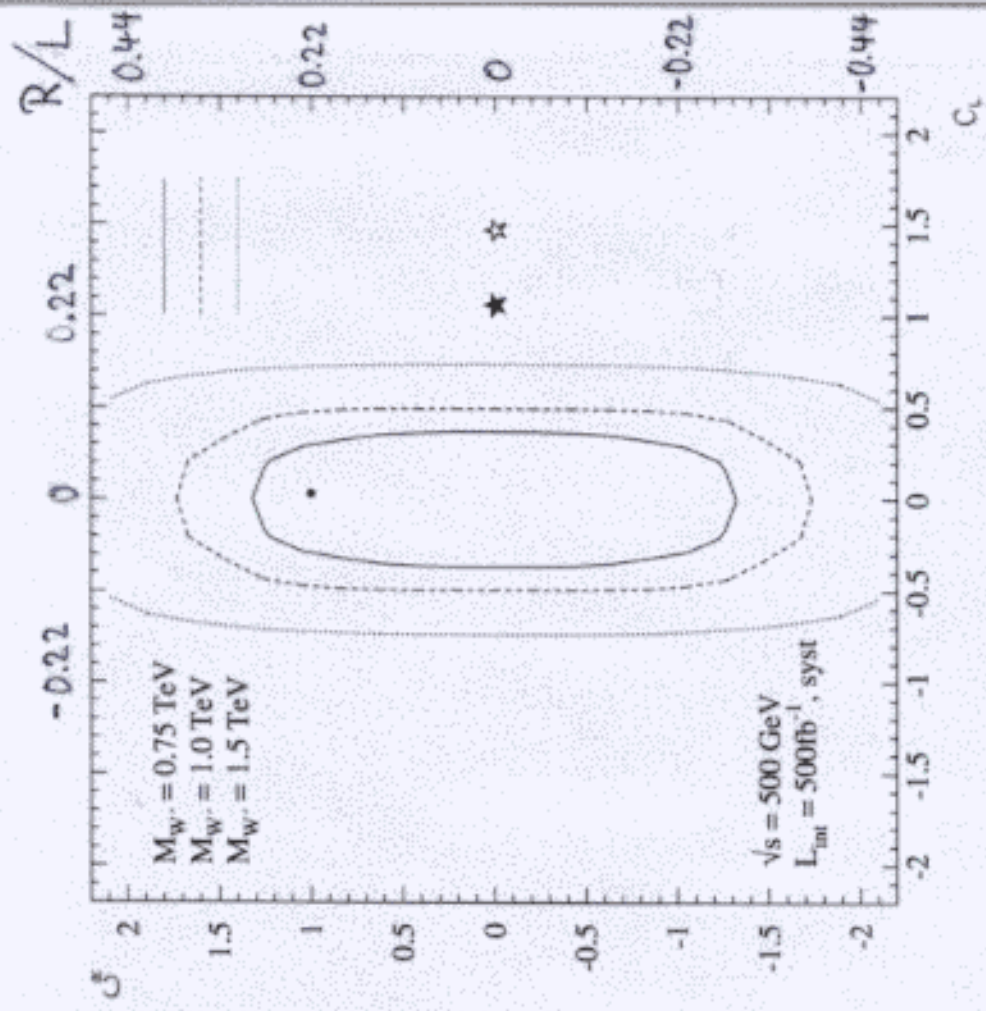
Model	$\sqrt{s} = 0.5 \text{ TeV}, L_{int} = 1000 \text{ fb}^{-1}$				$\sqrt{s} = 1 \text{ TeV}, L_{int} = 1000 \text{ fb}^{-1}$			
	$e^+e^- \rightarrow \nu\bar{\nu}\gamma$		$e\gamma \rightarrow \nu q + X$		$e^+e^- \rightarrow \nu\bar{\nu}\gamma$		$e\gamma \rightarrow \nu q + X$	
	no syst.	syst.	no syst.	syst.	no syst.	syst.	no syst.	syst.
SSM $W'$	5.1	1.7	4.8	2.7	6.3	2.2	6.9	4.6
LRM	1.3	0.9	0.8	0.6	1.8	1.2	1.3	1.1
KK	5.5	1.8	6.8	3.8	6.9	2.3	9.8	6.5

Table 3:  $W'$  discovery limits in TeV, see text.

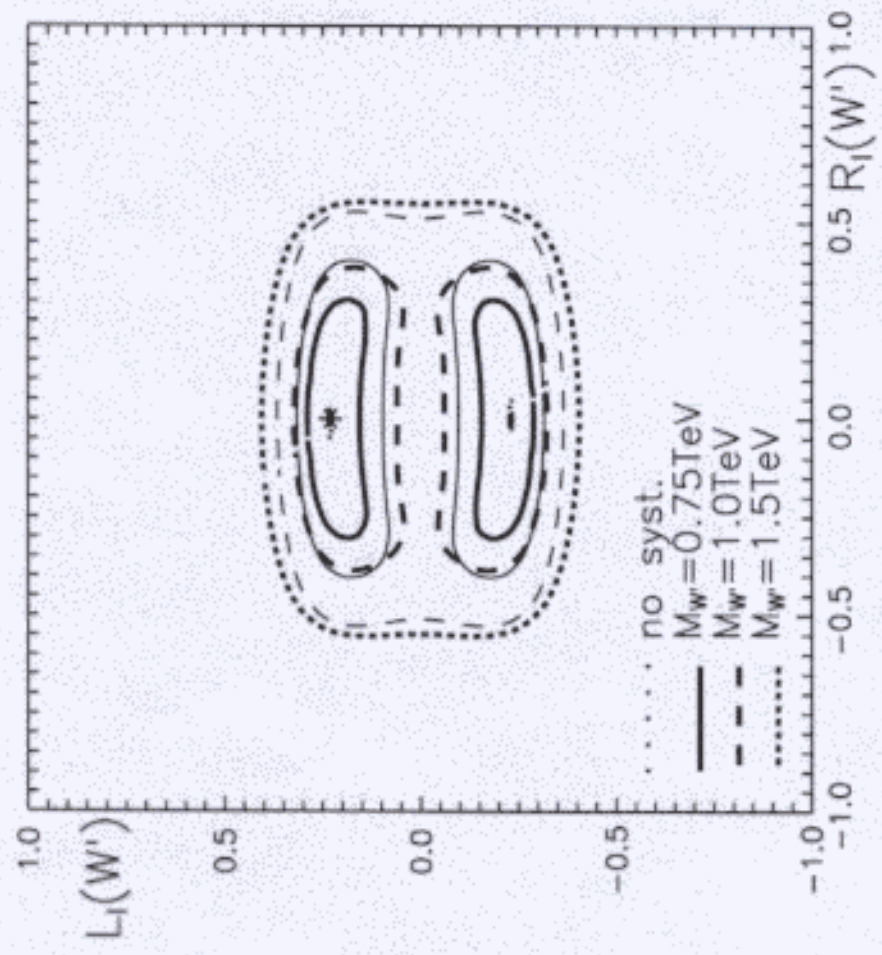
↙ syst. error < 2 (1) %

## References

[1] S. Godfrey, P. Kalyniak, B. Kamal, A. Leike, Discovery and Identification of Extra Gauge Bosons in  $e^+e^- \rightarrow \nu\bar{\nu}\gamma$ , Phys. Rev. D61 (2000) 113009, hep-ph/0001074.  
 [2] M. Doncheski, S. Godfrey, P. Kalyniak, B. Kamal, A. Leike, Discovery and Identification of Extra Gauge Bosons in  $e\gamma \rightarrow \nu q + X$ , hep-ph/0008157, subm. to Phys. Rev. D.



$e\gamma \rightarrow \nu\gamma$



$e^+e^- \rightarrow \nu\bar{\nu}\gamma$

# → HIGH PRECISION PHYSICS : Extended gauge sym.

## $E_6$ Leptons and SO(10) Neutrinos

Spira

i)  $E_6$  leptons. Twelve new fermions are needed to complete the 27 dimensional fundamental representation of  $E_6$ . They consist of two weak isodoublet leptons, two isosinglet neutrinos, which can be either of the Dirac or Majorana type, and an isosinglet quark appearing in a left- and a right-handed state:

$$\begin{bmatrix} \nu_E \\ E^- \end{bmatrix}_L \quad \begin{bmatrix} \nu_E \\ E^- \end{bmatrix}_R \quad N \quad N' \quad D_L \quad D_R \quad (17)$$

These particles can be pair produced via gauge boson exchange including a new  $Z'$  boson related to an additional abelian factor in the gauge group structure at low energies. The cross sections for pair production of the heavy charged and neutral isodoublet leptons are rather large thus allowing for the discovery of these particles with masses close to the beam energy [1], as can be inferred from Fig. 11a.

ii)  $SO(10)$  neutrinos. The fundamental representation of the  $SO(10)$  gauge group contains 16 fermions, which consist of the 15 fermions of one family in the Standard Model (SM) and a right-handed neutrino, which is a singlet under the SM gauge group. Mixing between ordinary and heavy right-handed neutrinos induces new couplings, which allow for the single production of the latter. Due to the large contribution of the  $t$ -channel  $W$  exchange, single Majorana neutrinos can be produced with masses close to the total c.m. energy of the  $e^+e^-$  collider; for mixing parameters not too tiny,  $\xi \gtrsim 10^{-2}$ , the production rates are large enough for the states to be detected [2], see Fig. 11b.

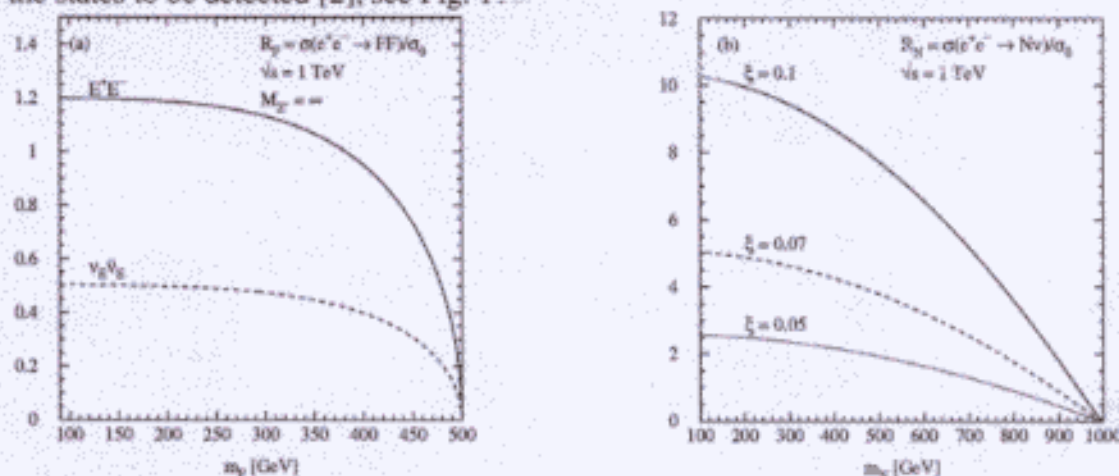
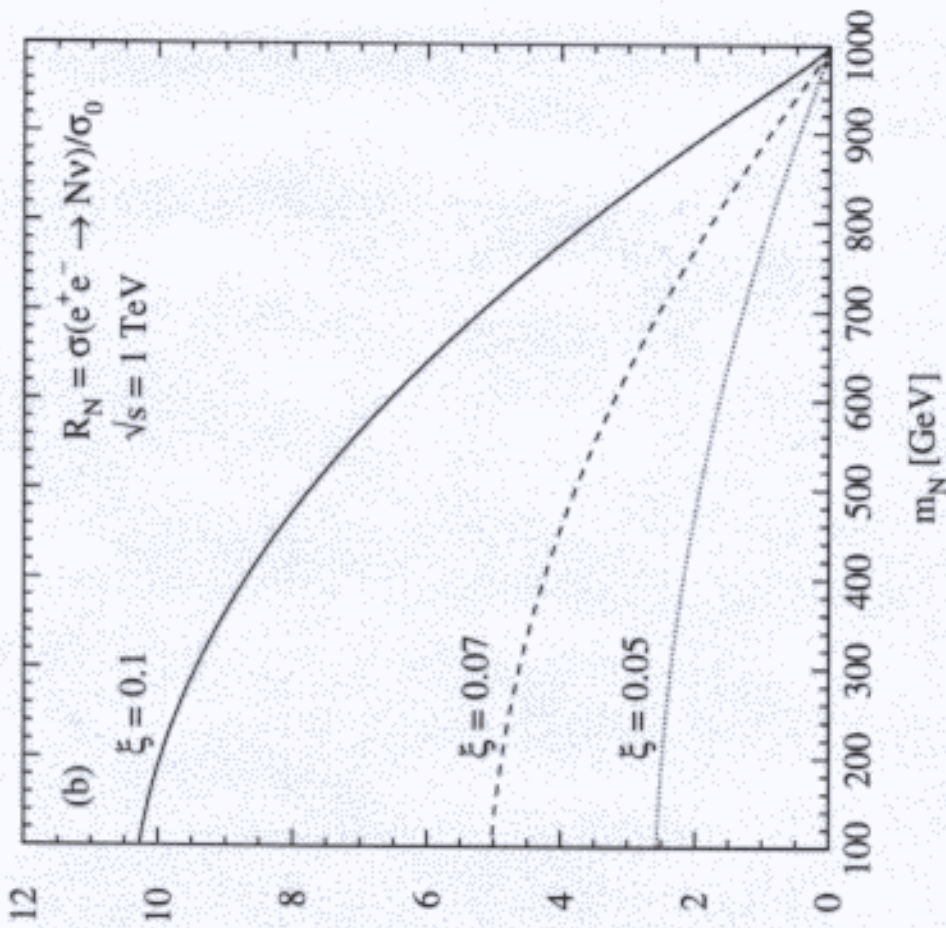
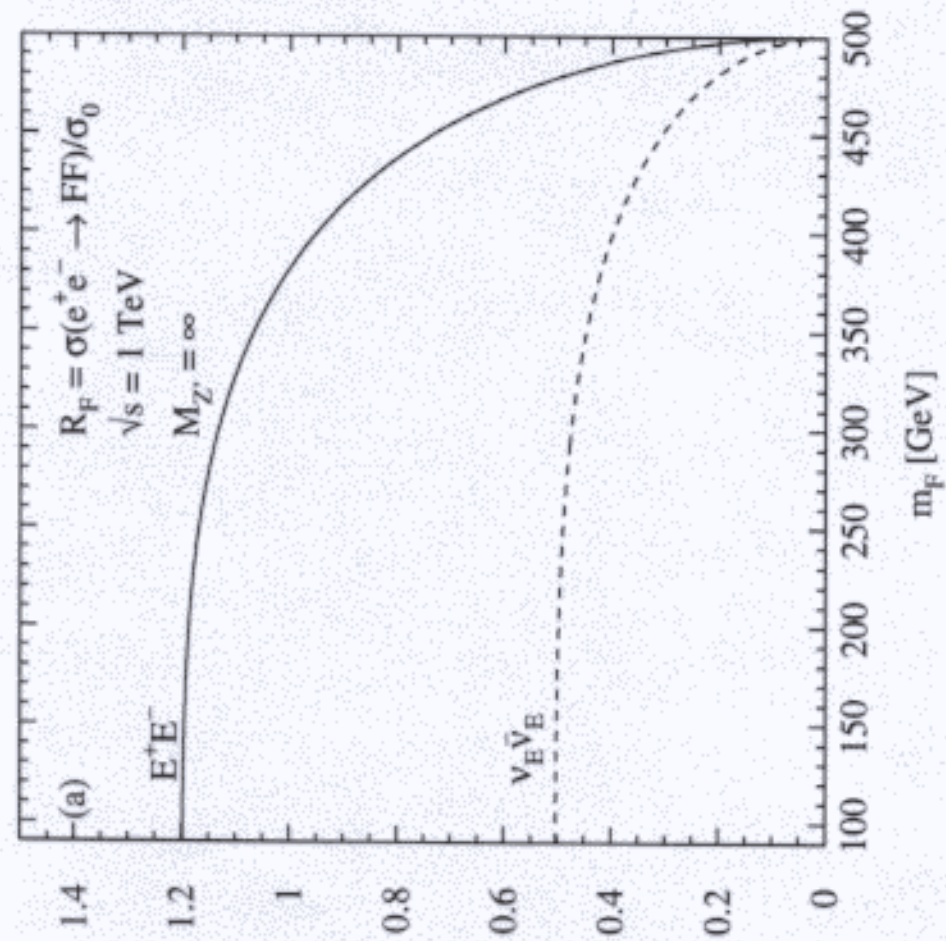


Figure 11:  $R$  values for (a) heavy  $E_6$  lepton pair production [without  $Z'$  exchange] and (b) single  $SO(10)$  Majorana neutrinos [for various mixing parameters  $\xi$ ] at  $\sqrt{s} = 1$  TeV.

$$\sigma_0 = \frac{4\pi\alpha^2}{3s} \approx 87 \text{ fb}$$

## References

- [1] J.L. Hewett and T.G. Rizzo, Phys. Rep. **183** (1989) 193 and references therein.
- [2] W. Buchmüller and C. Greub, Nucl. Phys. **B363** (1991) 345.



# → HIGH PRECISION PHYSICS

## 3.2.4 Chances for Precision Information on Heavy Majorana Neutrinos from the $e^-e^-$ Collider Heusch

Throughout the Linear Collider physics studies, there has been the consideration that, in its electron-electron version, this machine can give unmistakable and irrefutable evidence for the existence of TeV-level Majorana neutrinos, should Nature have chosen to account in this way for the deficiencies of the Standard Model neutral-lepton sector. Recent evidence on possible neutrino oscillations has done little to clear up the broader picture of (1) the Majorana vs. Dirac character of the neutrinos and (2) the disparity of masses of charged vs. neutral fermions in higher symmetry schemes.

We have pointed out that the exchange of TeV-level Majorana neutrinos in high-energy scattering of left-handed electrons can lead to clear signals in the reaction  $e^-e^- \rightarrow W^-W^-$ . In addition, the energy dependence of those signals gives precise information on mass and couplings of the exchanged Majorana neutrino.

Recent discussion has centered on the assertion that (a) such a process is excluded due to the non-observation of neutrinoless double beta decay, and (b) the greatest sensitivity to the possible existence of heavy right-handed singlets is offered by new and recently proposed experiments involving large tanks of double-beta-decay candidates such as germanium.

This contribution points out that, to effect such neutrinoless double beta decay, two  $d$  quarks from two different neutrons in the parent nucleus have to approach within  $< 10^{-10}$  cm, which leads to strong suppression by the color Coulomb barrier: if the two  $d$  quarks are in a spin singlet, color sextet configuration, their interaction is repulsive, and will be suppressed by a factor of order 100. If they are in a spin triplet, color anti-triplet state, this is attractive: but it takes a  $\Delta$  inside the decay candidate nucleus to accommodate the color anti-triplet, leading to a suppression factor of 50–80, to be multiplied by the usual color factor of three.

Moreover, we point out that even if there were a signal from a monoenergetic  $e^-e^-$  emission into a large germanium tank, no information would be available for the process that is responsible for it. The exchange of various supersymmetric particles, of specific types of leptoquarks, all with a great variety of couplings and of unknown masses would be candidates, just as the TeV Majorana neutrinos. The Linear Collider is the one venue for cleanly interpretable experimentation, where the energy and helicities of the incoming electrons provide for clean identification and definition of the exchanged heavy neutral lepton.

$0 \rightarrow \beta\beta$   
↓

to be merged with ....

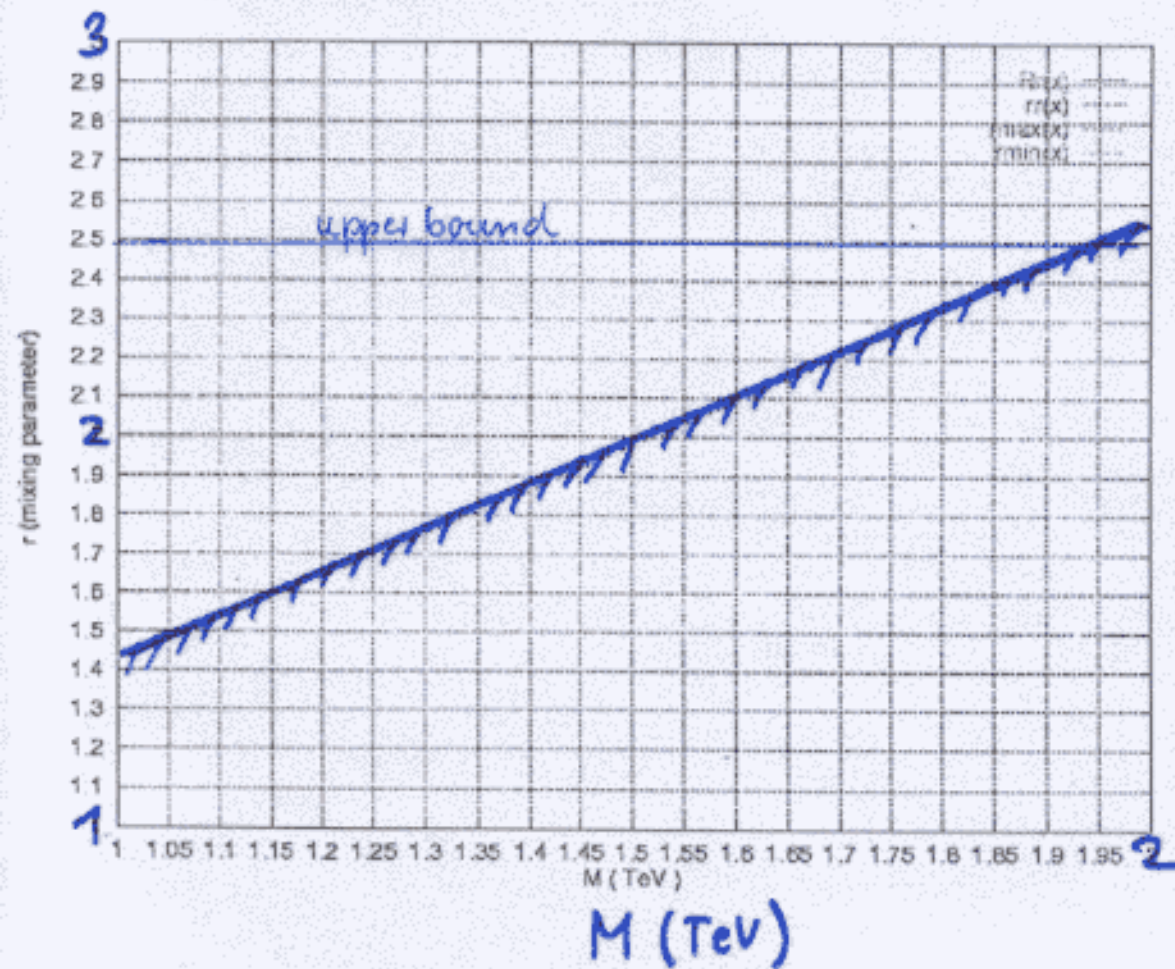
Minkowski

It is shown that the polarized  $e^-e^-$  mode of a linear collider operating at  $\sqrt{s} = 500 \text{ GeV}$  and an effective integrated luminosity of  $500/\text{fb}$  provides a discovery potential for a heavy neutrino flavor through the detection of the reaction  $e^-e^- \rightarrow W^-W^-$  depending on a favorable but allowed range of the heavy light flavor mixing parameter  $|U_{e\bar{h}}^2| = r (2 \cdot 10^{-4})$ ;  $1.5 \leq r \leq 2.5$ . The corresponding mass range for the heavy neutrino mass is  $M \leq 1.05 \text{ TeV}$  for  $r = 1.5$  and  $M \leq 1.95 \text{ TeV}$  for  $r = 2.5$ . For a mass of 1 TeV the coupling strength  $r$  has to exceed 1.4.

## References

- [1] P. Minkowski, *Int. J. Mod. Phys. A* **11** (1996) 1591.
- [2] C. Greub and P. Minkowski, *Int. J. Mod. Phys. A* **13** (1998) 2363.
- [3] C. Heusch and P. Minkowski, *Int. J. Mod. Phys. A* **15** (2000) 2429.





$$\uparrow \frac{|U_{eh}|^2}{2 \cdot 10^{-4}}$$

$$\sqrt{s} = 500 \text{ GeV}$$

$$P_{e^-} = 1$$

$$\int \mathcal{L} = 500 \text{ fb}^{-1}$$

$$\# \text{ ev.} = 8$$

$$\sigma_{\text{min}} = 1.6 \cdot 10^{-2} \text{ fb}$$

Figure 1: Discovery potential for a heavy neutrino flavor in the coupling and mass parameter space  $r$ ,  $M$ . The range corresponding to  $1.5 \leq r \leq 2.5$  is shown as shaded region.

# CONCLUSION

referring only to processes / tests discussed

ALTERNATIVES	LC	LHC
strong WW int. vector reson. ( $> 1\text{TeV}$ ) pseudo-Goldstone b.	$\Lambda \sim 3\text{TeV}$ * * * * * ( $\gamma\gamma$ )	$\Lambda \sim 2\text{TeV}$ (* ) *
leptoquarks contact int.	couplings ( $e\gamma$ ) $\Lambda \sim 50 \div 100\text{TeV}$	discovery $< 1.5\text{TeV}$ $\Lambda \sim 25 \div 35\text{TeV}$
KK radiation KK exchange	$M \sim 10\text{TeV}$ $M \sim 10\text{TeV}$ ( $\gamma\gamma$ )	$M \sim 5\text{TeV}$ ?
$Z', W'$	couplings $M \sim 10\text{TeV}$ (ind.)	discovery $< 5\text{TeV}$
$E_6/SO(10)$ fermions	Leptons	quarks
R - SUSY	$LL\bar{E}$ ( $\tilde{\nu}$ )	$LQ\bar{D}$ ( $\tilde{q}$ )
LFV on Z reson.	* *	—
wide, invisible Higgs	* *	—
Majorana $\nu$	* * ( $e^-e^-$ )	—

## Contributions to LC Notes

LC-TH-1999-012

*The  $t$ - $cH$  Decay Width in the Standard Model*

B. Mele

LC-TH-1999-013

*The Lightest Pseudo-Goldstone Boson at Future  $e^+e^-$  Colliders*

R. Casalbuoni, A. Deandrea, S. De Curtis, D. Dominici, R. Gatto,  
J.F. Gunion

LC-TH-1999-015

*Anomalous  $\gamma$ - $\gamma H$  and  $Z\gamma H$  Couplings in the Process  
 $e\gamma \rightarrow eH$*

E. Gabrielli, V.A. Ilyin, B. Mele

LC-TH-1999-018

*The Electroweak Chiral Lagrangian Revisited*

A. Nyffeler

LC-TH-1999-020

*Study of the Anomalous Couplings at NLC with Polarized Beams*

R. Casalbuoni, S. De Curtis, D. Guetta

LC-TH-1999-021

*Resonant Single Chargino and Neutralino Versus Fermion-Antifermion  
Production at the Linear Collider*

S. Lola

LC-TH-1999-022

*Constraints on Couplings of Extra Gauge Bosons from  $e^+e^- \rightarrow \nu n \bar{\nu}$   
 $\gamma$*

S. Godfrey, P. Kalyniak, B. Kamal, A. Leike

LC-TH-2000-006

*$Z'$  Indication from New APV Data in Cesium and Searches at Linear  
Colliders*

R. Casalbuoni, S. De Curtis, D. Dominici, R. Gatto, S. Riemann

LC-TH-2000-007

*Predictions for  $Z \rightarrow \mu \tau$  and Related Reactions*

J. Illana, M. Jack, T. Riemann

LC-TH-2000-020

*Tests of the left-right Electroweak Model at Linear Collider*

K. Huitu, J. Maalampi, P. N. Pandita, K. Puolamaki, M. Raidal,  
N. Romanenko

LC-TH-2000-040

*Single Chargino Production at Linear Colliders*

G. Moreau

LC-TH-2000-041

*Single Chargino Production with R-Parity Lepton Number Violation in  
Electron-Electron and Muon-Muon Collisions*

M. Czakon, J. Gluza